ANL/AMD-18/1

Final Report for U.S. Department of Energy Fuels & Lubricants Project on Lubricant Technology – Innovation, Discovery, Design, and Engineering

Applied Materials Division

ANL/AMD-18/1

Final Report for U.S. Department of Energy Fuels & Lubricants Project on Lubricant Technology – Innovation, Discovery, Design, and Engineering

---

by
George Fenske, Nicholaos Demas, Layo Ajayi, Ali Erdemir,
Cinta Lorenzo-Martin, Osman Eryilmaz, Robert Erck, and Giovanni Ramirez
Applied Materials Division, Argonne National Laboratory

John Storey, Derek Splitter, Brian West, Todd Toops, Melanie DeBusk, Samuel Lewis,
Shean Huff, Eric Nafziger, John Thomas, Brian Kaul, and Jun Qu
Oak Ridge National Laboratory

Lelia Cosimbescu
Pacific Northwest National Laboratory

Brad Zigler and Jon Luecke
National Renewable Energy Laboratory

July 2018

FINAL

Research Performance Progress Report (RPPR)
For
U. S. Department of Energy – EERE/VTO/Fuels & Lubricants

Award Number:	ANL	WBS 5.2.0.102
	ORNL	WBS 5.2.0.403
	PNNL	WBS 5.2.0.602
	NREL	WBS 5.2.0.302
Project Title:	Lubricant Technology - *Innovation, Discovery, Design, and Engineering*	
Principal Investigators (PIs):	Project Lead (ANL)	George Fenske
	Thrust 1 Lead (ANL)	Layo Ajayi
	Thrust 2 Lead (PNNL)	Lelia Cosimbescu
	Thrust 3 Lead (ORNL)	John Storey
	PI (ANL)	Nicholaos Demas, Layo Ajayi, Ali Erdemir, Cinta Lorenzo-Martin, Osman Eryilmaz, Robert Erck, and Giovanni Ramirez
	PI (ORNL)	John Storey, Derek Splitter, Brian West, Todd Toops, Melanie DeBusk, Samuel Lewis, Shean Huff, Eric Nafziger, John Thomas, Brian Kaul, and Jun Qu
	PI (PNNL)	Lelia Cosimbescu
	PI (NREL)	Brad Zigler and Jon Luecke
Submission Date:	July 31st, 2018	
Recipient Organization:	Argonne National Laboratory Oak Ridge National Laboratory Pacific Northwest National Laboratory National Renewable Energy laboratory	
Project/Grant Period:	Start date: October 1st, 2016, End date: September 30th, 2018	
Reporting Period End Date:	June 30th, 2018	
Reporting:	FINAL REPORT	

George Fenske July 31st, 2018

Signature Date

Contents

Figures

Figures (Cont.)

Tables

Introduction

In 2016, the Vehicle Technologies Office (VTO) of the Department of Energy (DOE) issued a solicitation for the AOP Lab Call research in FY2017 on a number of topics related to vehicles. Topic 6A of the Lab Call focused on research related to advanced lubricants: "…*(in)* support of the lubricants program goal to, by 2020, demonstrate novel formulations for powertrain and driveline lubricants, compatible with new and legacy vehicles, to achieve at least a 4 percent real-world fuel economy improvement." Argonne National Laboratory (ANL) in collaboration with Oak Ridge National Laboratory (ORNL) and Pacific Northwest National Laboratory (PNNL) was awarded a 3-year multilab project on "Lubricant Technology - Innovation, Discovery, Design, and Engineering." Research on the project began in FY2017 at the three laboratories with industry participation; however, in FY2018, the project was terminated due to budgetary constraints.

The following is the final report for the project and highlights progress made during the first year of research. The report is divided into sections that highlight the following:

- Goals, objectives, milestones and deliverables
- Project highlights
- Outreach – publications, conferences, and reports
- Milestones accomplished
- Research progress

Project Overview: Approaches to improve fuel economy and reduce emissions by reducing parasitic friction losses often present unique challenges to the design and formulation of lubricants. In addition to reducing parasitic friction losses, the lubrication system must maintain reliability and durability of traditional engine and driveline components, as well as enable the implementation of non-traditional, transformational technologies. For example, under hydrodynamic conditions, the challenge for improving fuel economy is to balance the reduction in viscous frictional losses obtained with low-viscosity fluids with the increase in friction and contact severity (wear and failure) associated with such fluids. Under mixed and boundary conditions, the challenge is to identify approaches that yield both low friction and low wear.

Game-changing technologies often have unintended effects on reliability. For example, the need to protect emission control systems against poisoning by sulfated ash, phosphorus, sulfur (SAPS) compounds limits the amount of traditional anti-wear additives used to protect engine components. Dilution of lubricants by advanced fuels (e.g., Co-Optima) can potentially degrade friction and wear resistance and compromise durability. The use of gasoline direct injection (GDI) and turbocharging technologies that provide significant downsizing and fuel efficiency gains has unintended effects on low-speed pre-ignition (LSPI, also referred to as "stochastic pre-ignition") and generation of soot. LSPI can have devastating effects leading to catastrophic engine failure and is, in part, dependent on lubricant chemistry. Soot-like particles produced with GDI have been associated with premature wear of valve train components. All of these factors need to be fundamentally understood and addressed in the formulation of lubricants and the design of the engine and driveline surfaces.

A lubricant is a balanced mix of different chemical components (base fluids and additives) that combine to meet specific performance requirements for viscosity, lubricity, contaminant control, corrosion, and chemical degradation. Additives interact with other additives and surfaces to provide/sustain desirable

bulk properties to form surface films that provide low friction and protect against corrosion and wear. Reliable knowledge of the complex chemical and physical interactions between additives and components is required to properly formulate a lubricant. These interactions are sensitive to external factors such as temperature, pressure, and shear, as well as internal factors such as reactions with other additives and with contaminants such as diluted fuel and combustion products. The challenge to original equipment manufacturers (OEMs) for vehicles, additives, and oil is to formulate new lubricants that reduce parasitic friction losses while accommodating transformational concepts that use non-traditional alloys and coatings in more aggressive environments.

Historically, development of lubricants, additives, and other lubrication-related materials has been Edisonian in nature, which can be time-consuming and expensive. A more holistic approach is thus needed to accelerate the development of lubrication concepts—one that is based on a detailed understanding of how lubricants and surfaces interact and react to external stimuli. To this end, the project developed tools and models to predict how lubricants and surfaces interact; how these interactions affect chemical, mechanical, rheological, and tribological properties; and how these properties affect vehicle efficiency, reliability, and durability. Tools and models were developed in conjunction with the development of advanced technologies (e.g., base fluids, additives, and coatings) that show high potential to provide significant improvement in performance. Considerable attention was directed towards gaining improved understanding on how lubricants degrade or age, and designing lubrication systems that retain performance throughout the lifetime of the lubricant, e.g., times equivalent to fresh, 500, 5000, and 10,000 miles in a vehicle.

To carry out the research, the project took advantage of the diverse, complementary capabilities at ANL (lab-scale testing, characterization, technology development, and modeling), ORNL (engine validation, additive development, and characterization), and PNNL (base fluid and additive design and development), as well as, under a contract with ORNL, the National Renewable Energy Laboratory (NREL, ignition quality testing). The project included industrial participation by vehicle, additive, coating, and oil OEMs. ANL coordinated individual efforts by the Labs and industrial partners. A formal communication and project management plan was established during the first quarter. The management team included members from each Lab.

Project Goal/Objective: The primary goal of the project was to understand and develop lubrication technologies that, when deployed, provide sustainable improvements to further vehicle fuel economy by up to 4%. In engines, one obvious approach is the use of lower viscosity oils. This approach has been under development in industry for over two decades and has led to the continuous introduction of lower viscosity oils into the marketplace. Further reduction of oil viscosity will present many technical hurdles, among which are vulnerability of engine components to premature failure and adequate long-term performance of the lubricant. Furthermore, new engine concepts and technologies under development by OEMs (higher cylinder pressures, use of GDI, etc.) can compromise the effectiveness of engine lubricants in terms of friction and wear reduction. Meeting the rather challenging and aggressive goal of a 4% increase in fuel economy requirement, and doing so in a sustainable manner, require innovative developments and effective integration of base fluids, additives, and surface technologies. Such developments must be undergirded by a better understanding of the basic mechanisms of the lubrication of surfaces, as well as understanding and mitigation of potential failure mechanisms.

Specific goals for the project were as follows:

1) By 2020, identify and validate lubricant technologies that further a 4% fuel economy goal by:
    a) Reducing parasitic asperity and hydrodynamic friction losses by 25% and

b) Enabling reliable functionality of transformational technologies that improve engine thermal efficiency, including advanced Co-Optima fuels.
2) Reduce carbon emissions commensurate with fuel economy savings.
3) Maintain or improve the reliability and durability of engine and driveline components.
4) Ensure that candidate lubricants function with both legacy vehicles and new vehicles that incorporate advanced materials and coatings.
5) By 2020, validate projected vehicle fuel economy benefits of promising lubricant concepts by using experimental engine/vehicle dyno test data.

Project Thrusts/Tasks: Lubricant research was performed collaboratively at four national laboratories (ANL, ORNL, PNNL, and NREL) with industrial stakeholder input and feedback. The research consists of three interrelated thrusts using core capabilities identified within the DOE Office of Energy Efficiency and Renewable Energy (EERE) VTO Lab capability matrix:

1) Surface and Lubricant Interactions – further our understanding of surface and lubricant interactions, including long-term oil aging/degradation effects on lubricant performance.
2) Technology Innovation, Design, and Synthesis – develop advanced base fluids, additives, and materials/coatings that reduce parasitic friction losses.
3) Engine and Vehicle Validation – validate lubricant effects on efficiency, after-treatment efficiency, and stochastic pre-ignition (SPI).

Specific tasks include:

Thrust/Task	Thrust/Task Title	Labs
1	**Surface & Lubricant Interactions**	
1.1	Innovative Methodologies for Rapid Evaluation of New Lubricant Technologies	ANL
1.2	Surface Characterization of Tribochemical Films	ANL
1.3	Development of Mechanistic Models of Lubrication	ANL
1.4	Coating/Lubricant Interactions	ORNL
1.5	Oil Aging and Degradation	ANL, ORNL
2	**Technology Innovation, Design & Synthesis**	
2.1	Lubricant Base Fluids	PNNL, ANL
2.2	Additives	PNNL, ANL
2.3	Materials and Coatings	ANL
3	**Lubricant Effects on Combustion and Emissions Control**	
3.1	Lubricant Effects on Emissions and Emission Controls	ORNL
3.2	Lubricant Effects on Low-Speed Pre-Ignition (LSPI)	ORNL, NREL
3.3	Lubricant Effects on Fuel Economy in Vehicle Experiments	ORNL

Each task involved industrial participation by vehicle, additive, coating, and oil OEMs. Each Lab developed teaming arrangements through non-disclosure agreements (NDAs), cooperative research and development agreements (CRADAs), etc., with their preferred industrial team. The teaming arrangements included:

Lab	Industrial Team
ANL	Ford and Infineum
ORNL	Cummins, Lubrizol, Driving Racing Oils, Shell, GM
PNNL	Afton Chemical, Shell Lubricants
NREL	N/A – NREL activities coordinated through ORNL

Due to the proprietary nature of lubricant and additive development, open exchange of data and intellectual property among all the labs and industrial partners was limited. To overcome this, each national laboratory partner developed teaming arrangements with their preferred industrial team members. Data and material provided by a given partner that had been designated to be proprietary were treated as confidential under an NDA. Data/material were not shared with others (e.g., during periodic project reviews with other national laboratory and DOE sponsor review meetings) without prior consent from the industrial partner.

The Lubricant Technology project as originally proposed was a 3-year multilaboratory project with 16 project-level milestones/deliverables, as shown in the table below. Due to termination of the project at the end of FY2017, only those milestones with dates in FY 2017 were completed (highlighted in **BOLD**, blue shading).

PROJECT LEVEL MILESTONES

Type	Number	Thrust	Milestone Description	Lab	DATE	Status
Regular	**1**	**1,2**	**Develop criteria, select baseline configuration (2009/GF4, or 2015/GF5), and identify pathways (base fluids, additives, and coatings) to pursue**	**All**	**FY17 Q2**	**COMPLETED**
Regular	**2**	**1**	**Complete development of test methodology for evaluating ring-on-liner scuffing performance**	**ANL**	**FY17 Q4**	**COMPLETED**
Regular	3	1	Develop and validate mechanistic scuffing model for engine components	ANL	FY19 Q1	CANCELED
Regular	4	1	Optimize coating and lubricant interactions for low friction and wear protection using common test protocol	ANL	FY19 Q2	CANCELED
SMART	**5**	**1**	**Quantify effect of engine oil ageing on tribological performance of engine oil**	**ANL, ORNL**	**FY18 Q2**	**COMPLETED**
Regular	6	2	Identify and evaluate base fluid concepts that exhibit suitable rheological performance (CCS, K_{40}, K_{100}, and HTHS) in desired grades (xx/16 and xx/12)	ANL, PNNL	FY18 Q4	**COMPLETED**
Regular	7	2	Synthesize and evaluate friction and wear performance of candidate AW/FM concepts (soluble and colloidal forms)	ANL, ORNL, PNNL	FY18 Q2	**COMPLETED**
Regular	8	2	Quantify the friction and wear reduction of ionic liquid containing formulation in a bench test versus GF5 baseline oil	ORNL	FY18 Q3	CANCELED
SMART	9	2	Demonstrate compatibility of an advanced coating with baseline (GF5) lubricant technology	ANL	FY18 Q4	CANCELED
Regular	**10**	**3**	**Quantify lubricant amounts in exhaust during cold start**	**ORNL**	FY17 Q3	**COMPLETED**
Regular	**11**	**3**	**Evaluate vehicle lube screening protocol using modern down-sped GDI engine-equipped vehicle**	**ORNL**	FY17 Q3	**COMPLETED**
Regular	**12**	**3**	**Develop correlation between IQT and engine studies of LSPI**	**ORNL, NREL**	FY17 Q4	**COMPLETED**
Regular	13	3	Evaluate prototype oil formulation from partner laboratory for comparison to Base Lube and commercial off-the-shelf lube for fuel economy improvement	ORNL	FY18 Q3	CANCELED
Regular	14	3	Identify catalyst effects for down-selected additives on TWC reactivity and material properties from Thrust II partners at Argonne and PNNL	ORNL	FY18 Q4	CANCELED
SMART	15	1, 2, 3	Compile and compare lubricant performance metrics (friction, wear, scuffing, degradation, emission degradation, LSPI, and fuel economy) as determined by lab-scale and vehicle tests	ALL	FY19 Q4	CANCELED
Go/No Go	16	1, 2, 3	Identify and demonstrate state-of-art low-viscosity lubricant systems that reduce friction by 20% over baseline (GF5/ferrous) without reducing wear performance	ANL, ORNL, PNNL	FY18 Q2	CANCELED

Project Highlights

1. A major focus of the Thrust 1 was on developing a scientific understanding of underlying tribological phenomena that determine friction and wear behavior, i.e., how lubricants and the additives interact with materials to form tribochemical films and affect the overall efficiency and durability/reliability of an engine. Project highlights from the five tasks on surface-lubricant interactions include:
    a. Development of a laboratory-scale test protocol to evaluate scuffing of ring and liner components. In collaboration with researchers from Daimler, an adjustable angle reciprocating tribometer (AART) test rig was designed and fabricated by using components from a traditional horizontal reciprocating rig. The AART unit not only had capabilities to control load, speed, and temperature similar to traditional horizontal test rigs, but also allowed the reciprocating table to be tilted to avoid puddling of oil at the interface. It also used an oil pump to precisely control flow of oil to the reciprocating interface at rates comparable to oil transport rates observed or predicted in fired engines. A series of shakedown tests using the AART rig confirmed the sensitivity of scuffing to load, speed, temperature, and oil supply rate. Proprietary research with a leading OEM successfully replicated/ranked the performance of oils in fired engine tests.
    b. Data on the structure and chemistry of thin protective tribochemical films that form during tribological interactions. A series on liner segments extracted from fired engines was examined to determine the nature of the films as a function of location along the liner. We found that formation of the tribofilms was non-uniform along the stroke length of the engine liner. Extensive formation of a film was found in the top dead center (TDC) region, but no film in the bottom dead center (BDC) region. The tribofilms studied had an amorphous and nano-crystalline phase mixture; hence, they were durable in protecting the ring and liner surfaces.
    c. Identification of the different wear modes that were active in the power cylinder. Detailed characterization of liner segments extracted fired engine tests revealed the presence of different modes of tribofilm failure depending on the location. Fatigue, abrasive, and scuffing modes of wear were observed. Removal of the tribofilm was a necessary condition for scuffing initiation on the liner.
    d. Determination of the effect of aging on performance by both Argonne and Oak Ridge researchers. Argonne worked with passenger car motor oil (PCMO) lubricants supplied by Infineum (aged in taxi fleet studies), while Oak Ridge worked with heavy duty diesel engine oil (HDDO) lubricants doped with carbon black (CB) to simulate the effect of diesel soot particulate. The Argonne studies showed a minor effect of aging on boundary friction. Wear was also impacted, but no clear trends were apparent due to early cancellation of the project. The work at Oak Ridge demonstrated that the wear behavior of CB-doped lubricants was strongly influenced by the presence of zinc dialkyldithiophosphate (ZDDP) as well as the composition of the test coupons.

2. Thrust 2 activities focused on technology development – specifically the development of base fluids, additives, and coatings. Project highlights for the technology development tasks include:
    a. Lipophilic polymethacrylate ionic liquids were prepared via scalable methods; among the synthesized compounds, a polymer bearing a dicyanamide anion showed an 85% reduction in wear versus non-ionic homopolymer, while all compounds displayed competitive viscosity indexes well above 200 at 5% concentrations in base oil.

b. Composite fluids consisting of a binary mixture made of polyalphaolefins (PAOs), different esters, and advanced hydrocarbons all showed a negative viscosity deviation, which may be amenable to empirical thermodynamic modeling.

Outreach – Publications, Conferences, & Reports

Publications:

1. L. Cosimbescu, B. Bhattacharya, R. Erck, S. Krueger, A. Martini, U.S. Ramasamy, J. W. Robinson, and B. J. Tarasevich, "High Efficiency Lubricant Oils and Additives Research," Annual Report PNNL-26104 (2016).
2. L. Cosimbescu, J. W. Robinson, J. T. Bays, and B. H. West, "Modified Thermoresponsive Hyperbranched Polymers for Improved Viscosity and Enhanced Lubricity of Engine Oils," Annual Report PNNL-26105 (2016).
3. J.W. Robinson, Y. Zhou, J. Qu, J.T. Bays, and L. Cosimbescu, "Highly Branched Polyethylenes as Lubricant Viscosity and Friction Modifiers," *Reactive and Functional Polymers* 31: 109:52-5 (2016)
4. George Fenske, Oyelayo Ajayi, Maria de la Cinta Lorenzo Martin, Ali Erdemir, Osman Eryilmaz, Nicholaos Demas, Robert Erck, and Giovanni Ramirez, "Lubricant Technology Development," DOE/VTO/F&L Annual Progress Report (FY 2016).
5. Nicholaos G. Demas, Robert A. Erck, and George R. Fenske, "Lab-Engine Prediction and Correlation," DOE/VTO/F&L Annual Progress Report (FY 2016).
6. Oyelayo Ajayi, Cinta Lorenzo-Martin, and George Fenske, "Phenomenological Modeling of Lubricant Film Formation and Performance," DOE/VTO/F&L Annual Progress Report (FY 2016).
7. Nicholaos G. Demas, Robert A. Erck, Cinta Lorenzo-Martin, Oyelayo O. Ajayi, and George R. Fenske, "Experimental Evaluation of Oxide Nanoparticles as Friction and Wear Improvement Additives in Motor Oil," *Journal of Nanomaterials*, Article ID 8425782, https://doi.org/10.1155/2017/8425782 (2017).
8. D. Splitter, "Impact of Engine Lubricant and Fuel Properties on LSPI," DOE/VTO/F&L Annual Progress Report (FY 2016).
9. John M. E. Storey, Todd J. Toops, Melanie M. DeBusk, Samuel A. Lewis, William Brookshear, and Eric A. Nafziger, "Lubricant Effects on Emissions and Emissions Control Devices," DOE/VTO/F&L Annual Progress Report (FY 2016).
10. Chao Xie, Todd J. Toops, Michael J. Lance, Jun Qu, Michael B. Viola, Samuel A. Lewis, Donovan N. Leonard, and Edward W. Hagaman, "Impact of Lubricant Additives on the Physicochemical Properties and Activity of Three Way Catalysts," *Catalysts* 6(4): 54 (2016).
11. Y. Zhou and J. Qu, "Ionic Liquids as Lubricant Additives – A Review," *ACS Applied Materials & Interfaces* 9: 3209-3222 (2017).
12. D. Splitter, B. Kaul, J. Szybist, and G. Janata, "Engine Operating Conditions and Fuel Properties on Pre-Spark Heat Release and SPI Promotion in SI Engines," *SAE Int. J. Engines* 10(3):2017, doi:10.4271/2017-01-0688.
13. W. Guo, Y. Zhou, X. Sang, D.N. Leonard, J. Qu, J.D. Poplawsky, "Atom Probe Tomography Unveils Growth Mechanisms of Wear-Protective Tribofilms Formed by ZDDP, Ionic Liquid, and Their Combination," *ACS Applied Materials & Interfaces* 9: 23152-23163 (2017).
14. Y. Zhou, D.N. Leonard, W. Guo, and J. Qu, "Understanding Tribofilm Formation Mechanisms in Ionic Liquid Lubrication," *Scientific Reports* 7: 8426 (2017).
15. L. Cosimbescu, N. Demas, J.W. Robinson, and R.A. Erck, "Friction and Wear Reducing Properties of Multifunctional Small Molecules," *ACS Applied Materials & Interfaces* 10(1): 1317-1323 (2018).
16. L. Cosimbescu, A. Vellore, U.S. Ramasamy, S.A. Burgess, and A. Martini, "Low Molecular Weight Polymethacrylates as Multi-functional Lubricant Additives," *European Polymer Journal* 104: 39-44 (2018).

Conferences & Presentations:

1. Cinta Lorenzo-Martin and Oyelayo Ajayi, ”Determination of Rheological Properties of Composite Base Fluid for Lubricants,” presented at Tribology Frontiers Conference, Chicago, IL (October 2016).
2. Dae-Kun Kim, Ke Nguyen, D. William Brookshear, and Todd J. Toops, “Impact of Lubricant Oil Additives on the Performance of Pd-Based Three-Way Catalysts,” presented at the 25th North American Catalysis Society Meeting (NAM).
3. Dae-Kun Kim, Ke Nguyen, D. William Brookshear, and Todd J. Toops, “Comparison of the Impact of Ionic Liquid and ZDDP Anti-wear Lubricant Additives on the Reactivity of Three-Way Catalysts,” presented at the 2017 SAE World Congress.
4. Y. Zhou, B. Stump, H. Luo, J. Qu, "Compatibility Between Anti-Wear Additives and Bronze and Aluminum Bearing Alloys,” presented at STLE 72nd Annual Meeting, Atlanta, May 21-25, 2017.
5. R. A. Erck, N. G. Demas, and G. R. Fenske, “Enhanced Analysis of Benchtop Friction and Wear Measurements” presented at STLE 72nd Annual Meeting, Atlanta, May 21-25, 2017.
6. N. G. Demas, R. A. Erck, and G. R. Fenske, “Novel Method for the Determination of Wear of Engine Cylinder Liner Parts” presented at STLE 72nd Annual Meeting, Atlanta, May 21-25, 2017.
7. O. O. Ajayi and C. Lorenzo-Martin, “One More Step Closer to Better Understanding of Boundary Lubrication Mechanisms,” Keynote presentation at 21st International Conference on Wear of Materials, March 26-30, 2017, Long Beach, CA.
8. O. O. Ajayi and C. Lorenzo-Martin, “Enhancement of Bronze Surface Properties by FSP and Second Particles Incorporation,” presented at 21st International Conference on Wear of Materials, March 26-30, 2017, Long Beach, CA.
9. C. Lorenzo-Martin, O. O. Ajayi, A. Erdemir, and R. Wei, “Tribological Performance of Quaternary CrSiCN Coatings under Dry and Lubricated Conditions,” presented at 21st International Conference on Wear of Materials, March 26-30, 2017, Long Beach, CA.
10. O.O. Ajayi, C. Lorenzo-Martin, and D. Singh “Tribological Performance of Carbon-Ceramics Composite Materials,” presented at STLE Annual Meeting & Exhibition, May 21-25, 2017, Atlanta, GA.
11. C. Lorenzo-Martin, O.O. Ajayi, A. Erdemir, and G. Fenske; “Friction and Wear Performance of Low-Viscosity Synthetic Mixed Fluids,” presented at STLE Annual Meeting & Exhibition, May 21-25, 2017, Atlanta, GA.
12. SAE 2016 International Powertrains, Fuels & Lubricants Meeting, Baltimore, MD, October 2016, Panel: Role of Lubricants in Reducing Energy Consumption and Emissions — Technical Challenges and Opportunities.
13. Y. Zhou and J. Qu, "Investigation of the Compatibility between Anti-wear Additives and Non-ferrous Bearing Alloys,” presented at 2016 STLE Tribology Frontiers Conference, November 13-15, 2016, Chicago, IL.
14. A. H. Shaw, J. Qu, R. D. England, and C. Wang, “Tribological Study of Diesel Piston Skirt Coatings in CJ-4 and PC-11 Engine Oils,” presented at 21st International Conference on Wear of Materials, March 26–30, 2017, Long Beach, CA.
15. G. Ramirez, S. Kota, O. Eryilmaz, Y. Gogotsi, M. Barsoum, and A. Erdemir, “Friction and Wear Behavior of MXenes under Dry Sliding Conditions,” presented at 41st Intl. Conference on Advanced Ceramics and Composites, January 22–27, 2017, Daytona Beach, FL.
16. G. Ramirez, B. Yonke, M. McCray, D. Schubert, and A. Erdemir, “Novel Borate Ester Additives with Superior Tribological Performance,” presented at 2016 STLE Tribology Frontiers Conference, November 13–15, 2016, Chicago, IL.
17. G. Ramirez, O. L. Eryilmaz, B. Narayanan, Y. Liao, G. Kamath, S. Sankaranarayanan, and A. Erdemir, “Investigation of the Tribocatalysis Mechanisms involved in the Extraction of Amorphous Carbon

Boundary Films from Base Oils, presented at 44th International Conference on Metallurgical Coatings and Thin Films, April 25, 2017, San Diego, CA.

18. Dae-Kun Kim, Ke Nguyen, D. William Brookshear, and Todd J. Toops, “Impact of Lubricant Oil Additives on the Performance of Pd-based Three-Way Catalysts,” presented at the 25th North American Catalysis Society Meeting.
19. Dae-Kun Kim, Ke Nguyen, D. William Brookshear, and Todd J. Toops, “Comparison of the Impact of Ionic Liquid and ZDDP Anti-wear Lubricant Additives on the Reactivity of Three-Way Catalysts,” presented at SAE World Congress and Expo, April 4, 2017, Detroit, MI.
20. J.M.E. Storey, M.M. DeBusk, S.P. Huff, S.A. Lewis, F. Li, J.F. Thomas, and M. A. Eibl, “Characterization of GDI PM during Start-Stop Operation with Alcohol Fuel Blends,” presented at the Health Effects Institute Workshop, Effects of Fuel Composition on PM, December, 2016.
21. Oyelayo Ajayi (presenter), Cinta Lorenzo-Martin, G. Fenske, N. Demas, R. A. Erck, and Jun Qu, presented at Annual Merit Review, Washington, DC, Lab Call-Thrust 1.
22. . Ramirez, O.L. Eryilmaz, B. Narayanan, Y. LIAO, G. Kamath, S. Sankaranayanan, and A. Erdemir, “Investigation of the Tribocatalysis Mechanisms Involved in the Extraction of Amorphous Carbon Boundary Films from Base Oils,” presented at G 44 International Conference on Metallurgical Coatings and Thin Films, April 25, 2017, San Diego, CA.
23. Lelia Cosimbescu, N. Demas, R. Erck, A. Martini, U.S. Ramasamy, and A. Vallore, “Molecular Design Strategies to Achieve a Multifunctional Oil Additive,” presented at STLE Annual Meeting & Exhibition, May 23, 2017, Atlanta, GA.
24. Lelia Cosimbescu (presenter), Oyelayo Ajayi, Ali Erdemir, Levent Eryilmaz, Maria De La Cinta Lorenzo Martin, Giovanni Ramirez, George Fenske, and Ashlie Martini, Annual Merit Review, Washington, DC; Lab Call-Thrust 2.
25. C. Lorenzo-Martin, O.O. Ajayi, A. Erdemir, and G. Fenske; “Friction and Wear Performance of Low-Viscosity Synthetic Mixed Fluids,” presented at STLE Annual Meeting & Exhibition, May 21-25, 2017, Atlanta, GA.
26. Y. Zhou, H. Luo, and J. Qu, "Compatibility between Ionic Liquids-Based Lubricant Additives and Bronze and Aluminum Bearing Alloys,” presented at STLE 72th Annual Meeting & Exhibition, May 21-25, 2017, Atlanta, GA.
27. Giovanni Ramirez, Osman Eryilmaz, Yifeng Liao, Ali Erdemir, Badri Narayanan, Ganesh Kamath, and Subramanian Sankaranarayanan, “In-Depth Studies of the In-Operando Formation of Amorphous Carbon Tribofilms at Lubricated Interfaces,” Presented at the STLE Annual Meeting& Exhibition, May 21-25, 2017, Atlanta, GA.
28. Dae-Kun Kim, Ke Nguyen, D. William Brookshear, and Todd J. Toops, “Impact of Lubricant Oil Additives on the Performance of Pd-Based Three-Way Catalysts,” presented at the 25th North American Catalysis Society Meeting, June 4-9, 2017.
29. Y. Zhou, D.N. Leonard, W. Guo, and J. Qu, “Tribofilm Formation Mechanisms in an Ionic Liquid-Additized Lubricant,” presented at STLE 73rd Annual Meeting, May 20-24, 2018, Minneapolis, MN.

Meetings:

1. Teleconference with Infineum — availability of “generic” GF5 5W/30 lubricant for baseline tests.
2. Teleconference call with Ford clarifying test coupons representative of modern passenger spark ignited car.
3. October 2016, invited presentation to Ford Motor Company on recent LSPI findings.
4. October 2016, invited presentation to Aramco Services on recent LSPI findings.
5. October 2016, presentation to Toyota Motor Company of Japan on recent LSPI findings.
6. Splitter, D., Kaul, B., Szybist, J., and Janata, G., “an update on pre-ignition research at ORNL”, presented to General Motors, June 26, 2017 via Webex.

Milestones Completed

Milestone 1 (All): We developed criteria, selected a baseline configuration (2009/GF4 or 2015/GF5), and identified pathways (base fluids, additives, and coatings) to pursue. A report documenting the approaches to develop and down select candidate technologies to improve fuel economy was prepared and submitted. The results are summarized below:

Pathways/Technologies	Approach
Low viscosity and multifunctional fluids	Reduce viscous shear losses
High performance additives	Reduce boundary friction Improve durability/reliability
Low-friction, wear-resistant coatings	Reduce boundary friction Improve durability/reliability
Down-Selection Criteria	**Methodology**
Friction (Boundary & Mixed)	Level 1 & 2 reciprocating tests
Wear & Durability	Level 1 & 2 reciprocating tests
Reliability/Scuffing	Level 2 scuffing
Rheology	CCS, capillary, and HTHS
Emissions	Effects on particulate emissions and catalyst durability
Ignition Quality	Elucidate lube properties and fuel/lube interactions that exacerbate LSPI
Fuel Economy	Develop a vehicle-based protocol that can screen "resource conserving" oils and bridge Sequence Test results to mile-per-gallon improvements
Reference Materials	**Description**
Reference Oils	FF GF5 5W/30, API reference oils – lab specific
Hardware/coupons	Rings, pistons, liners

Milestone 2 (ANL): We developed a test methodology for evaluating ring-on-liner scuffing performance. Through a collaborative effort with members of the MIT Lubrication Consortium, ANL researchers modified a conventional reciprocating test rig to enable operation under tilted conditions with precise control of flow of oil to the interaction zone. The newly modified system (AART) was used to characterize the effects of oil composition, temperature, speed, load, and oil supply rate on the occurrence of scuffing using prototypical segments of rings and cylinder liners.

SMART Milestone 5 (ANL/ORNL): We quantified the effect of engine oil aging on tribological performance of engine oil. An antagonistic effect between soot and ZDDP has been discovered in the excessive wear process, and it has been further found to be alloy dependent. The critical elements in the hypothetical tribocorrosion have been identified to be carbon in the soot and molybdenum in the alloy. Results provide fundamental guidance in future development of lubricants and bearing materials.

Milestone 6 (PNNL): Polyalkyl-methacrylates (PAMAs) with low molecular weight were originally designed to function as self-standing multifunctional base oils, the first of their kind. Successful implementation would result in the development of base oils with elevated thickening efficiency and film-forming capabilities, thus reducing the need for additives such as viscosity index improvers, anti-wear additives, and friction modifiers. However, even at low molecular weights, these PAMA-based

compounds were too viscous to behave as self-standing base fluids, when in neat form. Alternatively, the polymers were evaluated as multifunctional additives. Homopolymers of dodecyl methacrylate, 2-ethylhexyl methacrylate, and co-polymers of functional methacrylates (polar) were synthesized via a free radical process. Results show that the best performing of the new polymers exhibit viscosity indexes and friction coefficients comparable to those of our benchmarks, far superior shear stability to our benchmarks (as much as 15x lower shear loss), and wear reduction significantly better than a typical viscosity modifier (lower wear volume by a factor of 2-3). The findings also suggest that the polarity and molecular weight of the polymers affect their performance; as a result, future synthetic strategies may enable this new class of additives to replace multiple additives in typical lubricant formulations.

[L. Cosimbescu, A. Vellore, U.S. Ramasamy, S.A. Burgess, and A. Martini, "Low Molecular Weight Polymethacrylates as Multi-functional Lubricant Additives," *European Polymer Journal* 104: 39-44 (2018)].

Milestone 7 (PNNL): Methacrylate-type ionic liquid (IL) monomers containing ammonium or imidazolium cations and two different counter-anions were synthesized and used as co-monomers to obtain functional PAMAs as viscosity index improver (VII) additives for lubricants. The structure of the IL, including the cation, the anion, and the spacer's length separating the IL from the methacrylate group, plays an important role in the resulting polymer solubility in PAO, the solution rheology, and the friction and wear behavior. Depending on the IL structure, VIIs containing up to 20 mol% IL are soluble in PAO (grade 4) and demonstrate friction and wear reduction compared to a conventional oil-soluble PAMA. Notably, wear volume reduction reached up to 80% compared to the oil-soluble control, poly(dodecyl methacrylate).

[Abhijeet P. Bapat, Robert Erck, Bryan Seymour, Bin Zhao, and Lelia Cosimbescu, "Lipophilic Polymethacrylate Ionic Liquids: Synthesis and Application," submitted to *European Polymer Journal.*]

In a parallel study, poly(methacrylate)-type ILs containing a quaternary ammonium cation and two different counter-anions were synthesized, and their efficiency as friction- and wear-reducing additives was evaluated. The results were compared to those of PAO solutions additized with a small molecule, non-polymeric ionic liquid, or non-ionic copolymers containing 2-(dimethylamino)ethyl methacrylate as the polar co-monomer. No clear correlation between polymer molecular weight and friction or wear behavior was observed. Unexpectedly, random IL copolymers led to lower wear volumes than their block counterparts. Polymers containing dicyanamide counter anion showed lower wear volume compared to those containing bis((trifluoromethyl)sulfonyl)imide anion, but neither displayed competitive performance. Surprisingly, the IL moiety studied had no beneficial effect on wear.

[Abhijeet P. Bapat, Robert Erck, Bryan Seymour, Bin Zhao, and Lelia Cosimbescu, "What is the Effect of Lipophilic Polymeric Ionic Liquids on Friction and Wear?" submitted to *Reactive & Functional Polymers*.]

Milestone 10 (ORNL): Cold-start operation is a major contributor to particulate matter (PM) emissions for gasoline direct injection (GDI) engines. For this milestone, PM was collected during repeated cold starts of a GDI engine operating on E10 certification fuel. A start cart apparatus with forced cooling was developed to enable repeated cold starts in a day. The apparatus was equipped with fuel flow measurement, and the exhaust was collected in a full flow dilution tunnel. Triplicate filters were collected over six cold starts. Three lubricants from the same manufacturer (Mobil One®) were used: 0W-20, 10W-30 (recommended), and 20W-50. Results showed that the organic carbon portion of

the PM was primarily lubricant and made up between 40 and 60% of the PM mass. The 20W-50 had the lowest contribution to cold-start PM.

[J.M.M. Storey, S.P. DeBusk, S.A. Huff, E. Nafziger, V. Prikhodko, and J.E. Parks, “Exhaust Particle Emissions from Gasoline Engines: Characterization and Approaches to Filtration,” Presented at Advanced Filtration Technologies Conference, Louisville, KY, American Filtration and Separations Society, April 2017.]

Milestone 11 (ORNL): Improved fuel efficiency for lubricating oils is based on the ASTM Sequence VI test, which is performed on an engine. The translation of the Sequence VI test results to actual vehicle fuel economy improvements is critical to the support of programs aimed at improving the fuel economy of both emerging and legacy vehicles. A series of transient and steady-state cycles was used to compare the Sequence VI lubricant to Mobil 1 5W-30 on four vehicles, including one equipped with a modern turbocharged GDI engine. The results were similar across all four platforms and showed fuel economy gains of 1-5%, with the biggest improvements occurring during low speed operation.

1. Research Progress: Thrust Area 1 - Surface & Lubricant Interactions
(Thrust Lead: O. Ajayi - ANL)

1.1: Surface & Lubricant Interactions: Innovative Methodologies for Rapid Evaluation of New Lubricant Technologies

PIs: N. Demas and R. Erck (ANL)

Task Details: The objective of this task was to develop and refine innovative methodologies for the rapid evaluation of new lubricant and material technologies and to correlate the performance of these technologies in real engines and powertrain systems with results from laboratory test techniques. The goal was to evaluate candidate solutions under a common set of conditions.

Task Progress: During FY2017, activity in this task focused on development of test protocols to replicate scuffing conditions in the power cylinder of a diesel engine. Working with Daimler researchers in Germany, we evaluated the effect of load, speed, temperature, and oil supply rate on the scuffing.

Careful examination of the information that can be obtained from performing tests using differing test configurations is needed to determine their usefulness in simulating the ring-on-liner contact and, consequently, their efficacy to evaluate lubricant technologies. Two commonly used test configurations are the ball on flat and cylinder on flat under reciprocating sliding. Both of these configurations are simpler than the ring-on-liner configuration and could be useful on certain occasions. Most tribological performance evaluations of new additives intended for engine applications are conducted with the ball-on-flat configuration. Even though a contact configuration cannot be used to evaluate lubricants containing solid nanoparticles to reveal wear mechanisms that would be anticipated when materials with different roughness, composition, and hardness are subjected to different contact pressures, it can be useful for the evaluation of lubricants that do not contain solid particles.

During FY2017, we evaluated a baseline conventional GF5 5W30 oil provided by Infineum. The tribological behavior of this oil was investigated over temperatures ranging from 22°C to 160°C, and the results were compared with off-the-shelf formulations. From the tribological tests, we found that for this oil, temperature had no substantial effect on the boundary coefficient of friction , which was approximately 0.11±0.01 for tests up to 4 hours. Minor variations were observed for the off-the-shelf formulations.

Additionally, during FY2017 we started to evaluate the cylinder-on-flat test configuration with 10 mm stroke length and 2 Hz reciprocating frequency for 1 hour over a range of contact pressures between 330 MPa and 790 MPa (p_{max} =1 GPa). This test generates a line contact similar to the ring-on-liner test configuration in terms of its ability to provide quantifiable wear. This investigation was conducted because the precise measurement of wear for realistic components with surface roughness and honing marks, as in the case of cylinder liners tested against piston rings, is difficult. From these tests, we concluded that significant wear volumes are not produced when using fresh oil; wear over the width of the profilometric scans could not be quantified, and any systematic appearance of wear on this scale could not be trusted. However, oils with various levels of contaminants collected at specified intervals (5,070 miles, 8,016 miles, 10,411 miles) showed significant differences in wear when compared to fresh oil in tests using the cylinder-on-flat test configuration. By contrast, the ball-on-flat test configuration showed no significant differences in either friction or wear. The boundary friction coefficient for both configurations was approximately the same for all oils.

Furthermore, we used the AART in the tilted configuration to investigate the effect of oil supply and, hence, replicate the starved contact condition that the top compression ring experiences at TDC. Tests showed that the amount of oil has a significant effect on the friction and wear behavior. A sensitivity study was performed to examine the differences between oil flow rates and tribological behavior. We found that 0.1 μL/min is at the limit of starvation, and during a load increase, it produced black streaks and led to severe material wear. An increase in the flow rate to 0.2 μL/min produced black streaks and led to small and often gradual removal of material, while 0.5 μL/min produced no black streaks and led to mild polishing. The liner surface for representative tests are show in Figure 1.1.1.

Figure 1.1.1. Micrographs of gray cast iron liner surfaces subjected to a scuffing load test at flow rates of (a) 0.1 μL/min, (b) 0.2 μL/min, and (c) 0.5 μL/min.

Conclusions:

- We investigated existing friction and wear test protocols to examine oil degradation, and concluded that the cylinder-on-flat test protocol cannot accurately assess wear and differentiate between fresh oils but can assess oils with high levels of contamination that have occurred due to oil degradation.
- The importance of oil starvation was demonstrated to better simulate the contact at TDC.

1.2: Surface & Lubricant Interactions: Surface Characterization of Tribochemical Films

PIs: O. O. Ajayi and C. Lorenzo-Martin (ANL)

Task Details: In a previous study, a relationship was established between the structure of tribochemical surface films ("tribofilms") formed from additives and tribological performance. This finding provides strategies for minimizing boundary friction while protecting the surface. Using a combination of different advanced analytical techniques such as focused ion beam/high resolution transmission electron microscopy (FIB/HRTEM), grazing incidence X-ray diffraction (GIXRD), micro X-ray fluorescence (μXRF), and X-ray absorption near edge structure (XANES), this task sought to determine the structures of the tribo-chemical surface films on in-use engine liner surfaces as well as bench-top test coupons with various advanced additive systems. The nano-mechanical properties of the surface tribochemical films were measured by a nano-indentation technique.

Task Progress: We obtained in-use engine liner hardware from different OEMs. The parts were from both custom engine tests and field-operated engines. There was no information on the details of the lubricant used during the running of the various engines. Nonetheless, the results of the analyses of the tribofilms from these engine liners will be extremely valuable with regard to lubricant technology development for legacy vehicles.

In all the engine parts, formation of a tribochemical film was observed in both the ring and the liner surfaces. The film formation on the liner was, however, non-uniform though the stoke length. In all cases, tribofilms were formed in the TDC region and none in the BDC region. Sometimes, limited tribofilms formed in the mid-stroke region; other times, no tribofilm formed in the mid-stroke region. This finding is somewhat expected since the TDC is under more severe contact, and its temperature is higher. This likely caused the extensive formation of a tribofilm to protect the surface. The mid-stroke region operates primarily under the hydrodynamic regime, and thus underwent limited formation of tribofilm, if any. The temperature at the BDC is relatively low, and hence, there was a lack of formation of tribofilm. Consequently, only the tribofilm in the TDC was analyzed.

Figure 1.2.1a shows an optical micrograph of a typical tribofilm on a honing plateau of a cast iron liner. The patchiness and non-uniformity of thickness in the tribofilm are apparent. It is also clear that the tribofilm is effective in protecting the surface even under a severe contact condition, as indicated by the pronounced presence of the honing grooves. Figures 1.2.1b and 1.2.1c show an SEM micrograph and EDAX spectra, respectively. As evident from Fig. 1.2.1c, the tribofilm is rich in S, P, Mg, and Ca, all of which are constituent of oil additives.

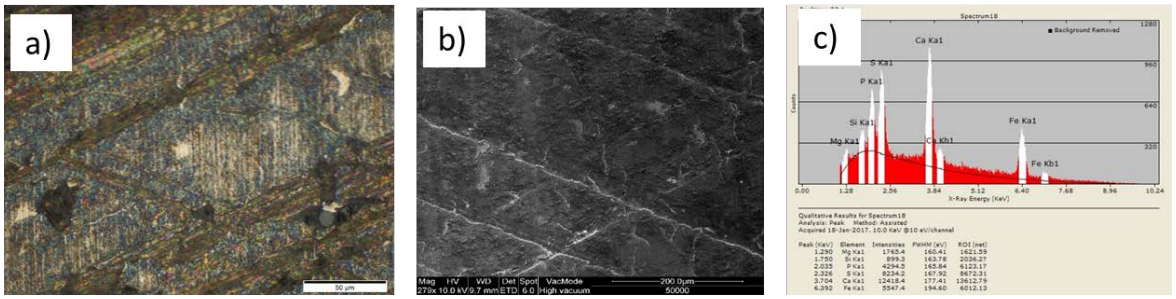

Figure 1.2.1. Surface of field-operated engine liner: (a) optical micrograph, (b) scanning electron microscopy (SEM) image, and (c) energy dispersive X-ray spectroscopy (EDAX) mapping of tribofilm.

Cross-sectional TEM analysis was conducted on several engine in-use tribofilms. The TEM samples were prepared by the standard FIB technique. Because of the fragility of the tribofilm, special care was taken to protect the surface during sample preparation. This involved first depositing a 10-50 nm gold layer, which coincidentally also acted as a marker during TEM analysis. Then, a total of about 1 micron platinum layer was deposited in two stages. This method protected the tribofilm from damage during FIB milling and thinning. The TEM analysis was conducted in a FEI Tecnai F20ST. Several analyses were conducted, including bright field and dark field imaging, scanning transmission electron microscopy (STEM), electron energy loss spectroscopy (EELS), EDAX, and selected area diffraction (SAED).

Figure 1.2.2a shows an overview of a tribochemical film from an engine. The thickness of the film is about 100-150 nm and appears to be non-homogeneous. The film is very well bonded to the substrate, as indicated by Fig. 1.2.2b. Nano-structurally, the films consist of nano-crystalline particles embedded in an amorphous phase. Based on our previous work, tribofilms with such a structure often exhibit relatively low friction and have very good durability. Hence, the film protects the surface against wear and severe damage, in spite of extreme contact conditions in the TDC region.

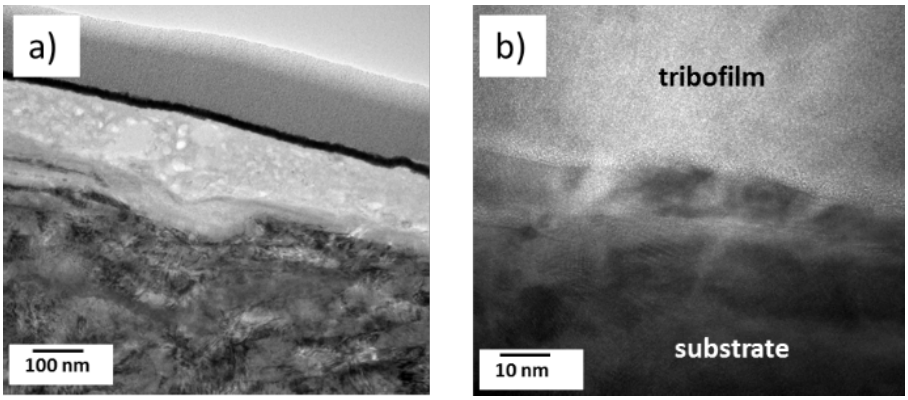

Figure 1.2.2. TEM micrograph of tribofilm: (a) overview and (b) substrate-film interface.

Figure 1.2.3 shows elemental mapping on the various constituent elements in the tribofilm. The figure clearly illustrates the non-uniformity of the composition and distribution of the various elements. Again, this is consistent with what is known about the complex nature of tribofilms.

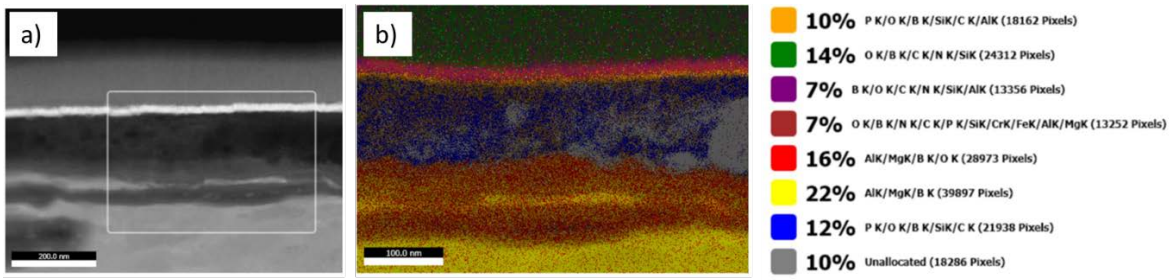

Figure 1.2.3. Tribofilm micrographs: (a) STEM and (b) EDAX elemental mapping

Summary:

- Formation of a tribofilm is non-uniform along the stroke length of the engine liner. Extensive formation of a film was found in the TDC region but no film in the BDC region.
- The tribofilms studied have an amorphous and nano-crystalline phase mixture; hence, they are durable in protecting the ring and liner surfaces.

1.3: Surface & Lubricant Interactions: Development of Mechanistic Models of Lubrication

PIs: O. O. Ajayi and C. Lorenzo-Martin (ANL)

Task Details: Adequate reduction in engine friction to achieve the project goal of fuel economy improvement will require the use of very low viscosity engine oils. As engine components operate under a boundary regime with introduction of ultra-low viscosity lubricants, they will be more susceptible to various failure modes. Accelerated wear and scuffing failures will be major issues that must be addressed to ensure reliability and durability of the engine. This task involves extensive failure analysis to determine the basic mechanisms of wear and scuffing in an engine ring-and-liner system. By use of a physics-of-failure approach, results of this task will be the basis for formulating a predictive model for engine wear and scuffing.

Task Progress: We obtained in-use engine ring-and-liner components with different degrees of wear and surface damage, including scuffing, from many OEMs. Some of the components are from engine tests for either wear or scuffing; others are from engines that failed in the field due to a variety of reasons. Various wear and damage modes were identified at different locations on the liner surface. One prominent mode was polishing and fatigue wear. This particular wear mode involves total smoothening of the honing plateau, as shown in Fig. 1.3.1a. In addition, wear by fatigue in the polished area is also evident by localized material removal in Fig. 1.3.1a. This wear mode appears not to involve extensive plastic deformation either on the surface or sub-surface regions, as indicated by Fig. 1.3.1b, which did not show much bending of the pearlite lamellae structure. Based on this observation, a linear elastic fatigue analysis was initiated in collaboration with MIT for the formulation of a predictive fatigue wear model.

The other prominent failure mechanism observed, especially in the TDC region, is scuffing. Analysis of various samples indicated that occurrence of scuffing is very well connected with the formation and removal of tribochemical surface films. In all cases observed in the engine hardware, initiation of scuffing was preceded by the removal of the tribochemical surface film (Figure 1.3.2a). Either independently or as a consequence, the removal of the tribofilm also coincided with severe plastic deformation of the near-surface material. Figure 1.3.2b shows the plastic strain pattern on a honing plateau of a cast-iron liner surface after complete removal of the tribofilm by ethylenediaminetetraacetic acid (EDTA) washing. Sub-surface microstructural analysis of the scuffed area also showed a layer of about 5-10 microns of extensive plastic deformation (Fig. 1.3.2c). In samples with severe scuffing, severe plastic deformation was indicated by the bending near the surface of the pearlite lamellae. There was also indication of “crumbling” of the cementite phase (Fe_3C) in the pearlitic microstructure (Fig. 1.3.2d). The broken cementite appears to be mechanically mixed with the ferrite to form a “metal-matrix composite” layer of about 25-micron thickness on the scuffed surface. Quantification of the near-surface strain field can be the basis for mechanistic model formulation for scuffing. If one assumes that scuffing in the liner cast iron material occurs by adiabatic shear instability, as was the case in steel material, it is possible to formulate a predictive scuffing model based on the critical shear strength for scuffing initiation.

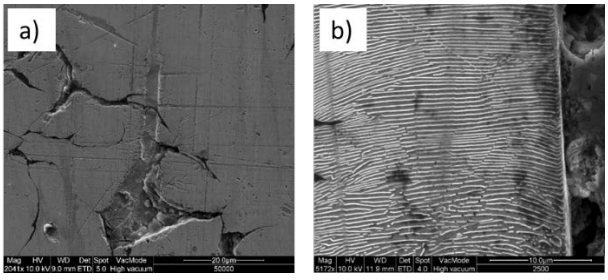

Figure 1.3.1. SEM micrograph of (a) polishing and fatigue wear and (b) sub-surface structure.

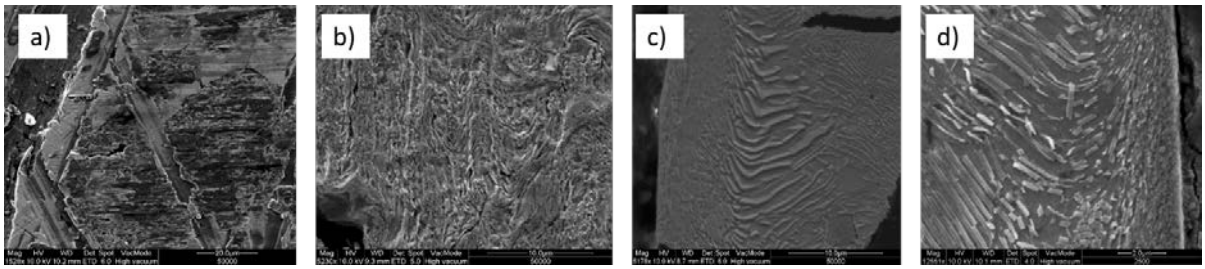

Figure 1.3.2. SEM micrograph of (a) local tribofilm removal, (b) plastic strain pattern on the surface, (c) sub-surface plastic deformation below scuffed surface, and (d) sub-surface structure after severe scuffing damage.

Summary:

- Different wear modes occur on the engine liner surface at different locations: fatigue, abrasive and scuffing wear modes.
- Removal of the tribofilm is a necessary condition for scuffing initiation on the liner.
- Scuffing involved severe plastic deformation of near surface material; a shear instability mechanism may be a viable approach to predictive modeling.

1.4: Surface & Lubricant Interactions: Coating/Lubricant Interactions

PIs: J. Qu, Y. Zhou, W. Li, and C. Kumara (ORNL)

Task Details: This study investigated the compatibility between engine oil additives, particularly anti-wear (AW) and friction modifier (FM), and non-ferrous bearing alloys and hard coatings. Its goal was to help guide future development of engine lubricants.

Task Progress: Tribological performance of a boundary lubrication contact is largely dominated by the FM and AW in the lubricant. While oil-soluble ILs have recently demonstrated promising anti-wear functionality, their compatibility with FMs is little known and even less understood for non-ferrous alloys. Here, we report the latest results of a compatibility study between four selected ILs and an organic friction modifier (OFM) for steel-bronze contact in boundary lubrication.

Depending on its chemistry, using an AW together with the OFM could be either synergistic or antagonistic, as suggested by the coefficient of friction , wear volume, and worn surface roughness shown in Table 1.4.1 and Fig. 1.4.1. The ZDDP additive seemed to slightly degrade the performance of the OFM. It may physically adsorb onto the bronze surface by the strong chelating effect between its sulfur atoms and the copper atoms, which inevitably are in competition with the OFM surface adsorption and thereby impair the integrity of the OFM surface film. The OFM seemed to not work well with the three aprotic ILs studied ([P8888][DEHP], [P66614][BTMPP] and [P66614][C17H35COO]), resulting in increased friction and wear. A strong intermolecular hydrogen bond and competitive adsorption between OFM and the aprotic ILs are believed to interfere with the self-assembly of the OFM molecules, causing deterioration in the surface film properties. In contrast, the protic IL ([N888H][DEHP]) showed a strong synergistic effect with the OFM, yielding an ultra-low steady-state friction coefficient (0.02-0.03) and wear rate ($<10^{-8}$ mm^3/N-m), significantly outperforming the OFM or the IL alone. Surface characterization of the bronze worn surface found no chemically reacted tribofilm, and thus, the superior tribological performance is hypothetically attributed to a physically adsorbed surface film constructed by the OFM and [N888H][DEHP] combination. Fourier transform infrared

spectroscopy analysis suggested that the N888 and HDEHP molecules in the IL may form intermolecular hydrogen bonds with the OFM molecules at a similar energy level as that among the OFM self-assembly. Thus, when the N888 and HDEHP are involved in the construction of the OFM surface film, they do not impair the film integrity but instead enhance the attraction with the metal surface by their higher polarity and the strength of the interactions among the OFM molecules created by the stronger hydrogen bonds, as illustrated in Fig. 1.4.2. As a result, the surface film becomes more difficult to compress vertically but easier to shear horizontally, leading to low friction and low wear.

Table 1.4.1. Summary of friction and wear results of OFM and OFM+AW

Lubricant (1 km sliding)	Final friction coeff.	Wear vol. ($\times 10^7$ μm^3)	Roughness (R_q, nm)	Compatibility
PAO4 + 0.8% OFM	0.075	2.48±0.82	167	-
PAO4 + 0.8% OFM+0.8% ZDDP	0.086	3.65±1.00	225	Antagonistic
PAO4+0.8% OFM+1.04% [P8888][DEHP]	0.137	8.39±2.00	493	
PAO4+0.8% OFM+0.99% [P66614][C17H35COO]	0.136	13.90±1.90	394	
PAO4+0.8% OFM+0.99% [P66614][BTMPP]	0.114	8.26±0.20	216	
PAO4+0.8% OFM+0.87% [N888H][DEHP]	0.032	0. 85±0.07	81	Synergistic
PAO4+0.8% OFM+0.87% [N888H][DEHP] 10 km	0.020	0. 82	87	
PAO4+0.87% [N888H][DEHP]	0.090	10.5±1.85	251	

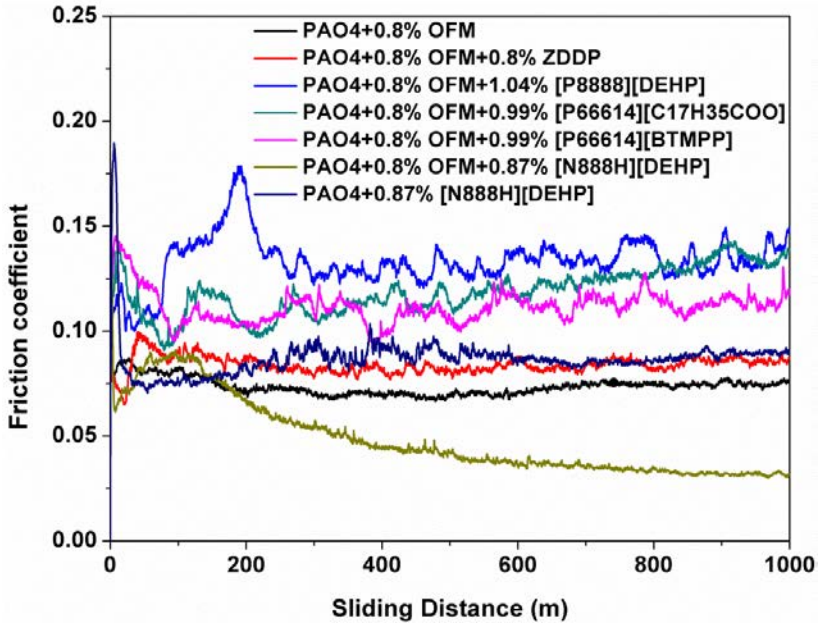

Figure 1.4.1. Friction coefficient traces of lubricants containing the OFM alone, OFM+ZDDP, and OFM+IL. The OFM and [N888H][DEHP] showed a strong synergistic effect, yielding an ultra-low friction coefficient.

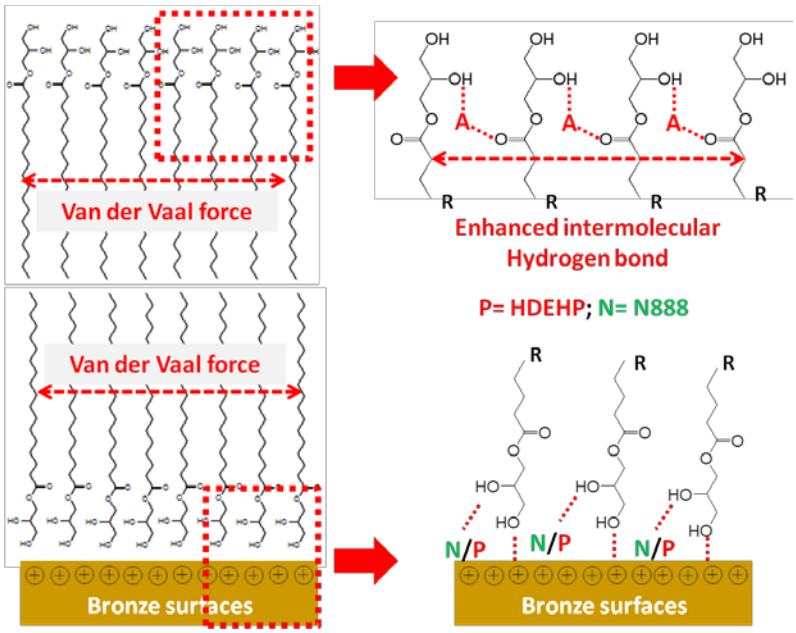

Figure 1.4.2. Schematic of tribological mechanism of combination of OFM and [N888H][DEHP]. The N888 and HDEHP are involved in the construction of the OFM surface film to enhance the attraction with the metal surface and strengthen the interactions among the OFM molecules.

1.5a: Surface & Lubricant Interactions: Oil Aging and Degradation (ANL)

PIs: O. Ajayi, C. Lorenzo-Martin, N. Demas, and R. Erck (ANL)

Task Details: Engine oils in vehicles are changed at regular intervals because the lubricant performance in terms of friction reduction and surface protection degrades with time. Oil aging and consequent loss of satisfactory performance occur by a combination of several mechanisms, including fuel dilution, shearing of viscosity index additives, oxidation, nitration, soot buildup, and loss of AW and FM additive efficacy. Oil aging changes different properties of the lubricant and often results in the loss of fuel economy gains. The objective of this task was to determine and quantify the impact of oil aging on the properties and tribological performance of engine oil. Attempts were made to secure an adequate number of data in terms of aging time to enable the formulation of an empirical model to predict lubricant properties and performance with time.

Task Progress: During FY2017, we secured several test oils, which had been operated in a spark-ignition engine for 5,070 miles, 8,016 miles, and 10,411 miles. Small quantities of oil had been removed from the engine at 5,070 miles and 8,016 miles. Larger quantities of fresh and 10,411-mile drained oil were available.

The viscosities of these test oils were measured at temperatures of 40° and 100°C. All the oils were consistent with SAE J300 specification 20 grade oil, which is required to have a kinematic viscosity between 5.6 and 9.3 cSt. During operation in the vehicle, the viscosity index degraded slowly with use, decreasing from 160 to 150, as shown in Table 1.5a.1.

Table 1.5a.1. Viscosity indexes for fresh oil and oil after operation in a spark-ignition engine run for 5,070 miles, 8,016 miles, and 10,411 miles.

Oil	Visc 40°C cSt	Visc 100°C cSt	Viscosity Index
Fresh	48.02	8.659	160
5,074 miles	49.87	8.64	152
8,016 miles	52.51	8.913	150
10,411 miles	53.93	9.11	150

Oil viscosity measurements were also performed for the fresh and 10,000-mile oil to determine if the required low-temperature cranking specifications were maintained. Because this test requires larger amounts of oil, the intermediate 5,000 and 8,000 mile oils were not used. As shown in Table 1.5a.2, the fresh and 10,000-mile oils maintain a low-temperature cranking viscosity of less than 6,600 cP at -30°C, thus verifying that they meet the specification for a 5W20 engine oil.

Table 1.5a.2. Viscosity indexes for fresh and 10,411-mile oils as function of temperature.

Temperature (°C)	-10	-15	-20	-25	-30	-35	-40
Fresh oil viscosity (cP)	418	682	1160	2307	4836	10710	24810
10,411 mile oil viscosity (cP)	571	909	1549	3079	6473	15150	36230

Ball-on-flat reciprocating tests were performed on the four oils at a temperature of 100°C, reciprocating frequency of 2 Hz, stroke length of 20 mm, and maximum Hertzian contact pressure of 1 GPa. The graph of coefficient of friction as a function of time (Fig. 1.5a.1) shows no systematic differences regardless of the usage history of the oil.

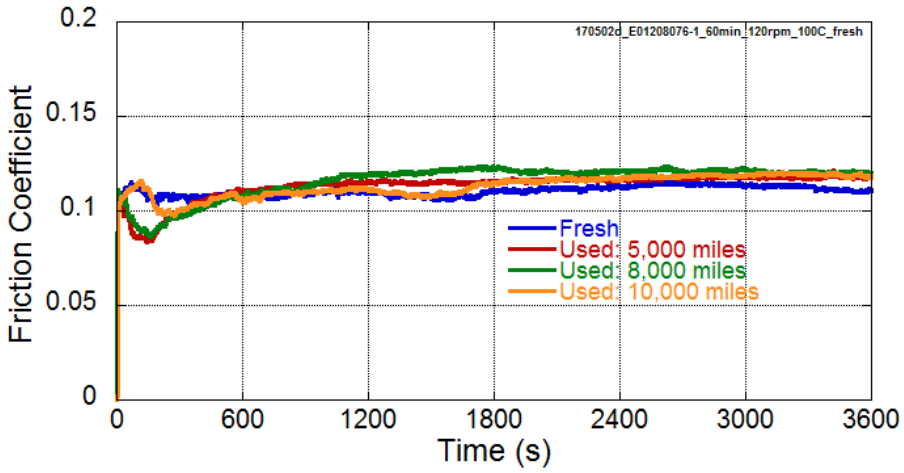

Figure 1.5a.1. Ball-on-flat coefficient of friction for the fresh and used oils

Pseudo-color and optical images of the flattened ball scars are shown in Fig. 1.5a.2 along with the measured amounts of wear. The optical images show the characteristic brown and blue/yellow of tribofilms from fully formulated oils. There is no discernable trend in the wear behavior.

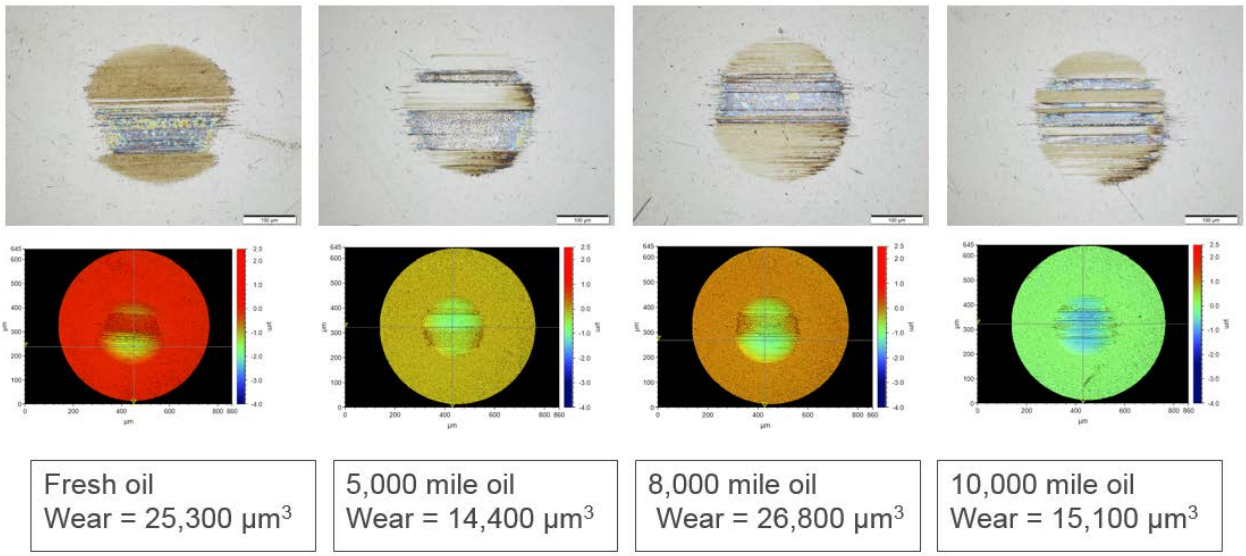

Figure 1.5a.2. Top: optical micrograph images of wear scars on the ball. Middle: pseudo-color 3D micrographs of wear scars. Bottom: degree of oil aging and associated wear volume.

1.5b: Surface & Lubricant Interactions: Investigation of the Wear Mechanism of Sooted Engine Oils
PIs: J. Qu, C. Kumara, Y. Zhou, and S. Lazarevic (ORNL)

Task Details: Soot in oils from gasoline turbocharged direct injection (GTDI) and diesel engines impacts the engine durability (higher wear rate) and fuel economy (higher oil viscosity). This study investigated the mechanism behind this well-known but little-understood problem of soot-accelerated engine wear.

Task Progress: Soot is generated from incomplete combustion of fuel during the engine combustion process, particularly in diesel and GTDI engines. These soot particles may be blended in the circulating engine lubricant oil or discharged into the environment. The soot content in the engine oil has been reported to strongly correlate with engine wear. The soot-induced wear mechanism, however, is lacking consensus. Several hypotheses have been proposed in the literature. Some studies observed antagonistic interaction between ZDDP and soot or carbon black (CB, as soot surrogate) while others did not. Considering distinct wear behavior reported for different steels, we suspected alloy dependency in the soot-induced wear process and, thus, conducted this study. The wear behavior and mechanism were investigated for four steel alloys in seven contact material pairs when lubricated by CB-containing oils with and without ZDDP.

The morphology of the CB particles is shown in Fig. 1.5b.1 (left) with particle sizes in the range of 50-100 nm. The wear results of the 52100 steel ball-M2 steel flat pair are shown in Fig. 1.5b.1 (right). As expected, adding the ZDDP alone (w/o CB) to the PAO oil effectively protected both the ball and flat, and blending the CB alone (w/o ZDDP) in the PAO oil caused significant wear increase for both contact surfaces. The ball wear was significantly higher than the flat wear, with a ratio (52100 steel ball wear/M2 steel flat wear) around 5:1 in the neat PAO base oil, PAO+ZDDP, and PAO+CB. However, when

both the ZDDP and CB were added to the base oil, the wear ratio between the ball and flat surprisingly flipped from 5:1 to 1:4, a 20X change. Basically, adding ZDDP into the PAO+CB oil protected the 52100 steel ball with a wear reduction of >70%, but increased the M2 steel flat wear by >5X. To our knowledge, no such observation has been previously reported in the literature. Tests were then conducted using the 52100 steel ball sliding against an A2 tool steel flat (different composition than M2 steel and less wear resistance), and similar wear behavior was observed. While the total wear volumes of the ball and flat were about the same when lubricated by PAO+CB and PAO+CB+ZDDP, the ball/flat wear ratio was reduced from more than 2:1 (CB alone) to less than 1:3 (CB+ZDDP), as shown in Table 1.5b.1.

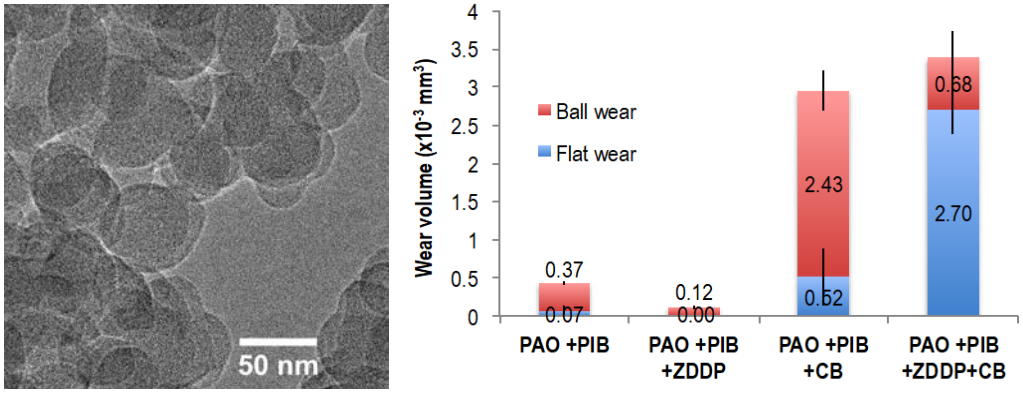

Figure 1.5b.1. (Left) Morphology of the CB used in this study. (Right) Wear volumes for 52100 steel ball against M2 tool steel flat in PAO containing ZDDP alone, CB alone, and both ZDDP and carbon black (CB).

Our results could not be explained by the recent hardness hypothesis proposed by Spikes, because the 52100 bearing steel, M2 tool steel, and A2 tool steel have similar hardness: 878, 876, and 821 HV, respectively. Instead, a combination of adhesive wear, abrasive wear, and catalyzed tribo-corrosive wear is proposed. In PAO+CB, the increased wear may be ascribed to the CB-induced abrasive wear and, consequently, adhesive wear due to significantly roughened contact surfaces, as revealed by the worn surface characterization. In contrast, the wear scars generated by PAO+CB+ZDDP appeared much smoother (see Fig. 1.5b.2) and, based on surface chemical analysis, are covered by significant amounts of tribochemical reaction products with ZDDP. This finding implies “tribocorrosion” on the M2 or A2 steel flat. The CB could act as a catalyst to trigger the tribocorrosion between ZDDP and the M2 or A2 steel surface, in a similar manner to the diamondlike carbon coating-catalyzed tribocorrosion reported earlier. But why did the 52100 steel ball have a wear reduction instead? Comparing the alloy compositions for the 52100 bearing steel with these two tool steels, we found that the prominent element is Mo, which accounts for 4.5-5.5% in the M2 steel and 0.9-1.4% in the A2 steel, but less than 0.1% in the 52100 steel. Thus, Mo seemed to be necessary for the hypothesized tribocorrosion.

To further understand the wear mechanism, five additional material pairs were tested: 52100 steel ball against 52100 steel and silicon nitride flats and M50 tool steel ball against 52100 steel, M2 tool steel, and silicon nitride flat. Results showed consistent wear reduction for the 52100 steel and wear increase for M-series tool steel when ZDDP was introduced to the CB-containing oil, which supported the Mo-involved tribocorrosion hypothesis. In summary, the wear behavior and mechanisms in the CB-containing oil highly depend on the presence of ZDDP as well as the compositions and mechanical properties of the two contact surfaces.

Table 1.5b.1. Summary of wear results tested in PAO+CB and PAO+CB+ZDDP.

Ball material	Flat material	Lubricant	Wear volume (x10^{-3} mm^3)			
			Ball	Flat	Ball/Flat	Total
AISI 52100 steel	AISI 52100 steel	PAO+CB	2.9±1.35	27.9±4.8	1.0E-01	30.8±5.0
		PAO+CB+ZDDP	3.2±0.50	NM*	3.2E+01	3.2±0.50
	A2 tool steel	PAO+CB	5.38±0.22	2.43±0.50	2.2E+00	7.81±0.54
		PAO+CB+ZDDP	1.68±0.07	5.84±0.06	2.9E-01	7.53±0.09
	M2 tool steel	PAO+CB	2.43±0.26	0.52±0.38	4.7E+00	2.95±0.46
		PAO+CB+ZDDP	0.68±0.35	2.70±0.31	2.5E-01	3.38±0.47
	Silicon nitride	PAO+CB	113±46	*Not measurable*	1.1E+03	113±46
		PAO+CB+ZDDP	14.7±6.1		1.5E+02	14.7±6.1

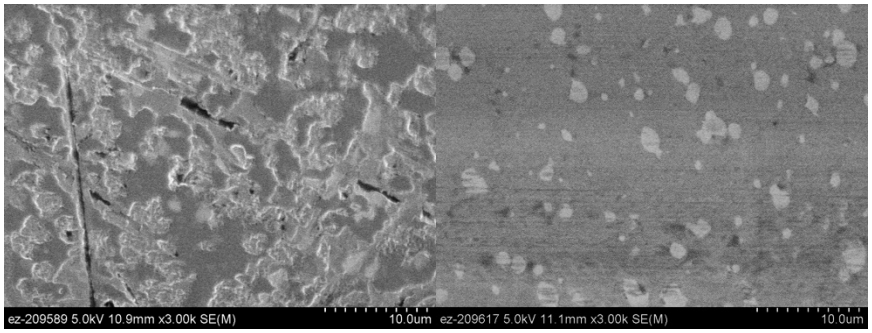

Figure 1.5b.2. The wear scars on the M2 flats lubricated by PAO+CB (left) and PAO+CB+ZDDP (right).

2. Research Progress: Thrust Area 2 - Technology Innovation, Design & Synthesis (Thrust Lead: L. Cosimbescu - PNNL)

2.1a: Technology Innovation, Design & Synthesis: Multifunctional Lubricant Base Fluids (PNNL)
PIs: L. Cosimbescu (PNNL)

Task Details: Polymethacrylates have been heavily explored for lubricant additive purposes because of their excellent thermal properties and stability. The same properties can be achieved in base fluids, if much lower molecular weight analogs are prepared. Linear polymethacrylates of various molecular weights and compositions were synthesized, as shown in Fig. 2.1a.1, and their rheological properties as neat oils evaluated.

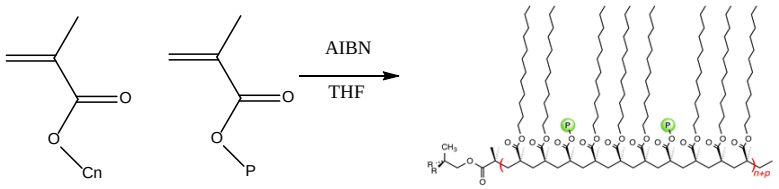

Figure 2.1a.1. Schematic showing synthesis of linear polymethacrylates

Task Progress: These compounds were too viscous to behave as self-standing base fluids when neat, so instead were treated as multifunctional additives. The synthetic approach is simple, clean, and scalable to obtain a product free of metals or sulfur. The polymers were added to 4Yubase at a fixed concentration of 12.5 wt.% and then characterized in terms of their viscosity-temperature behavior, shear stability, friction, and wear. Table 2.1a.1 captures the composition and viscosity properties of these blends.

Table 2.1a.1. Kinematic viscosity (KV) and viscosity index (VI) values for all polymer analogs and benchmarks studied

Sample	Composition	Concentration of polymer in 4Yubase	KV40 (cSt)	KV100 (cSt)	VI
4Yubase	100% 4Yubase		18.8	4.2	127
AW-1	$PA_{12}MA$-DMAEMA	12.5%	40.67	8.80	204
AW-2	$PA_{12}MA$-MEMA	12.5%	35.46	7.61	191
AW-3	$PA_{12}MA$	12.5%	40.83	9.52	228
AW-4	PEHMA	12.5%	45.06	8.98	185
AW-5	$PA_{12}MA$-EHMA-DMAEMA (low AIBN)	12.5%	55.53	12.00	219
AW-6	$PA_{12}MA$-EHMA-DMAEMA (high AIBN)	12.5%	40.06	8.5	196.8
B-1	PAMA	4.1%	55.42	12.0	274
B-2	PNNL polymer (fully formulated)	1.5%	55.5	12.0	219

In order to achieve VIs equivalent to commonly used viscosity modifiers, the polymers had to be added at rather large concentrations of 12.5%. Of the compounds explored in this work, samples AW-1, AW-3, and AW-5 have VIs of 191-228 and are comparable to B-2. An advantage of synthesized analogs is their potential superior shear stability owing to their low molecular weight. In contrast, viscosity modifiers can suffer substantial shear losses in a short time, which makes their high VIs irrelevant. To probe the stability of AW-1 to AW-6 under shearing, the Coordinating European Council (CEC) test method L45 was performed for 20 h at 100 °C against two benchmarks, B-1 and B-2, and the data are reported in Table 2.1a.2.

Table 2.1a.2. Shear stability data using the CEC L45 test method (20 h at 100 °C)

Sample	KV (cSt) before shear	KV (cSt) after shear	Viscosity Loss, %
AW-1	8.906	7.640	14.1
AW-2	7.745	7.550	2.45
AW-3	10.58	8.929	15.6
AW-4	9.039	8.696	3.76
AW-5	10.88	8.854	18.6
AW-6	8.538	7.828	8.31
B-1	34.13	10.80	68.3
B-2	12.47	6.504	47.8

The friction and wear properties of the different lubricant samples were evaluated at 100 °C under a load of 40 N in the boundary lubrication regime (sliding time was 1 h). The wear data show a distinct dependence on the ability of the polar co-monomer in the polymer to interact with the surface. The average (four runs) wear volume of the polymer compounds ranges from 121 to 367 x 10^3 μm^3, which is lower than the average wear exhibited by benchmark B-1 (375 x 10^3 μm^3) but higher than that of B-2 (31 x 10^3 μm^3). These observations are expected since B-2 is a fully formulated oil additized with ZDDP anti-wear package, while the other solutions contain base oil and polymer only, without an anti-wear package.

The lowest wear among the polymer analogs is exhibited by AW-1, AW-2, AW-4, and AW-6. Of these, the first three are the most polar of the six analogs tested, a finding that supports the hypothesis that polar polymers are more effective at reducing wear. However, AW-6, one of the more polar analogs tested, also exhibited lower wear. This may be explained by its relatively low molecular weight; the molecular weight of AW-6 is half that of the next smallest polymer. Therefore, these results indicate that low molecular weight and high polarity/propensity for surface interaction of the polymer may enable wear reduction. Although these additives were only in the early stages of development, they could be easily adoptable in a drop-in lubricant for the legacy fleet.

2.1b: Technology Innovation, Design & Synthesis: Ultra-low Viscosity Hybrid Base Fluid

PIs: C. Lorenzo-Martin and O.O. Ajayi (ANL)

Task Details: Engine friction can be reduced and fuel economy improved with lower viscosity engine oil. A synthetic, low-viscosity hybrid base fluid with optimized rheological properties can produce friction

reduction in the hydrodynamic regime without compromising performance in the boundary regime. This task was aimed at developing hybrid/composite base fluids with improved rheological and tribological properties, consisting of binary and ternary Group III-V fluid composites. Various rheological properties and tribological performance attributes of the hybrid fluids were evaluated with and without model additives.

Task Progress: Several binary ultra-low viscosity base fluids were formulated from PAO4, different forms of esters (polyol ester and diester), and advanced hydrocarbons (synthetic hydrocarbons). For the mixed fluids, we conducted comprehensive rheological performance measurements to determine the kinematic, cold crank, and high-temperature high-shear (HTHS) viscosities, as well as traction under slide/roll contact. Friction and wear performance were also determined under unidirectional and reciprocating contact. Standard four-ball testing of the lubricating capacity of the mixed fluids was also conducted. All the measurements and testing were done in comparison with a single-fluid constituent.

In general, the viscosity behavior shown in Fig. 2.1b.1 is typical for most of the mixed fluids tested, a finding that is consistent with the negative viscosity deviation principle. This translates to a reduction in hydrodynamic frictional loss in fluid film lubrication. Such a consistent observation of the rheological properties with the mixed fluids suggests they may be amenable to predictive modeling. Consequently, a data base of measured viscosity for various binary fluids has been initiated and could eventually be used for empirical thermodynamic predictive modeling of the rheological properties of hybrid base fluids with ultra-low viscosity. Once developed and validated, such a model would be a very useful tool for base-fluid technology development. The model could also have applications beyond lubricant development and formulation.

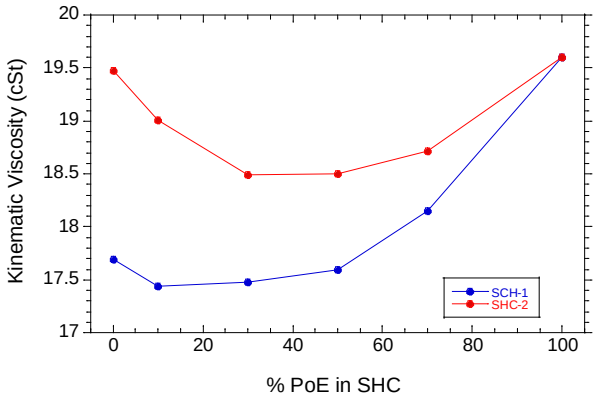

Figure 2.1b.1. Kinematic viscosity for binary ester-SHC composite fluids.

In spite of the viscosity reduction in mixed fluids, friction was notably reduced for the vast majority of the mixed fluid combinations. This was the case for PAO/ester mixtures, as well as superhard carbon (SHC)/ester mixtures. Figures 2.1b.2a and 2.1b.2b show examples of the average friction coefficient during unidirectional and reciprocating sliding of a steel ball on a steel flat, respectively, tested with SHC/ester mixtures. The minimum friction coefficient occurred with 10-25% ester concentration. Similar trends were observed for many other composite fluids. A much more dramatic difference was observed in wear performance. More than two orders of magnitude reduction in wear was observed with some composite base fluids when compared to single-constituent fluid. Figures 2.1b.2c and 2.1b.2d show the wear on the flat steel surfaces from unidirectional and reciprocating sliding test, respectively.

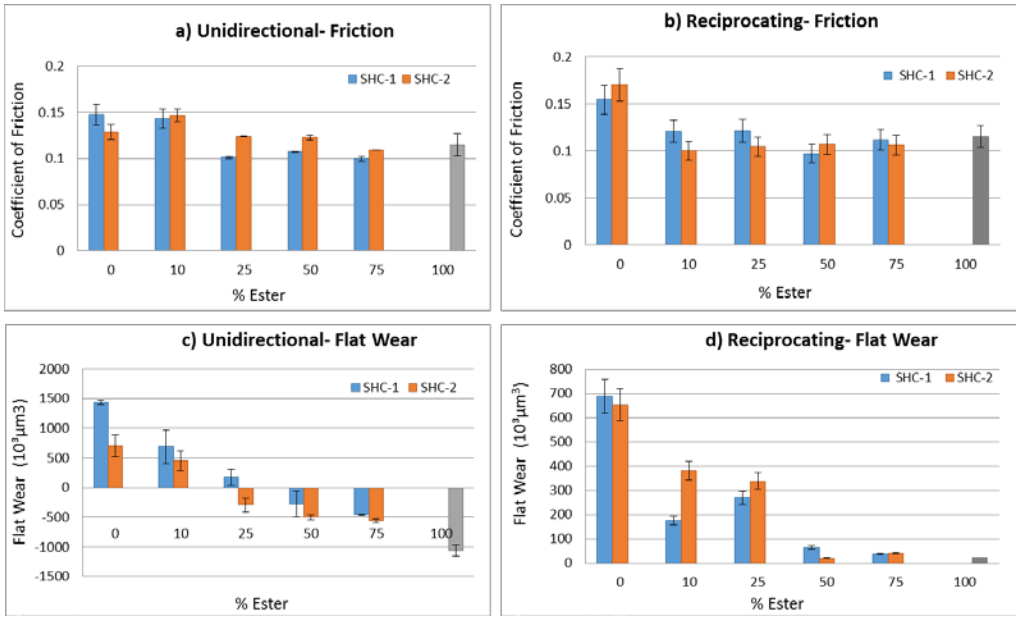

Figure 2.1b.2. Friction and wear measurement under unidirectional and reciprocating sliding as a function of ester concentration.

Under a more severe contact condition obtained in four-ball testing, all the mixed fluids reduced wear by 5-25 times compared to a single-constituent fluid, as shown in Fig. 2.1b.3. The superior tribological performance in term of friction and especially wear of mixed base fluids suggests that such fluids will be excellent candidates for formulation of ultra-low viscosity engine oils. Furthermore, such fluids may require lower levels of tribological performance additives, especially ZDDP, whose use is being curtailed.

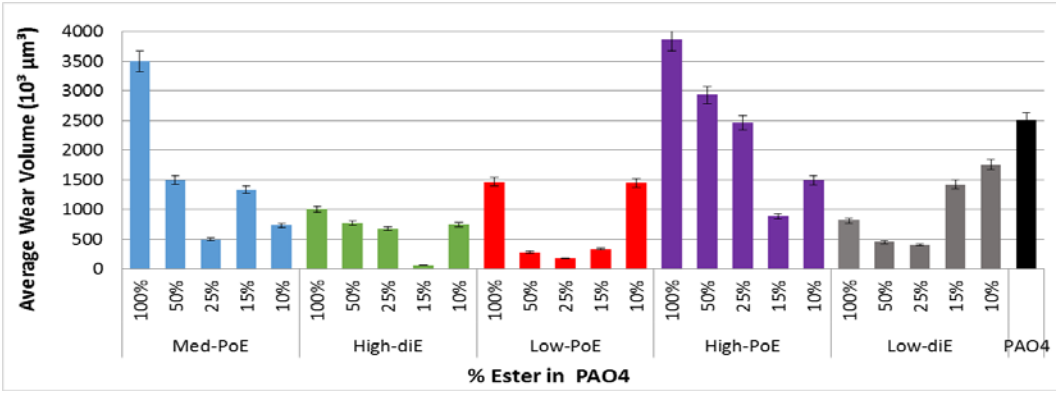

Figure 2.1b.3. Wear measurement under four-ball testing for binary ester-PAO4 composite fluids (PoE = polyol ester and diE = diester).

Task Summary:

- Composite fluids consisting of a binary mixture made of PAO, different esters, and advanced hydrocarbons all showed a negative viscosity deviation, which may be amenable to empirical thermodynamic modeling.
- Comprehensive tribological performance evaluation showed that mixed fluids exhibited noticeable friction reduction but very dramatic wear reduction compared to single-constituent fluids. This observation makes such fluids excellent candidates for ultra-low viscosity lubricant formulation.

2.2b: Technology Innovation, Design & Synthesis: Additives (PNNL)

PIs: L. Cosimbescu (PNNL)

***Task Details*:** The objective of this task was to combine polymer moieties that are known to improve the viscosity index with various functionalities that are known to be effective toward the reduction of friction and wear (ILs). Early experiments involved more easily accessible random copolymers to enable the selection of the best co-monomers. We designed and synthesized a large series of viscosity index improvers that covalently bind an IL moiety. For interest of space that work is not presented here, but a manuscript summarizing the work has been submitted to the *European Polymer Journal*. In a second phase of the project, similar IL moieties were incorporated in lower molecular weight polymers in an attempt to improve friction or wear, or both. For ease of synthesis, a di-block copolymer design was implemented to maximize the effect of the design and address the performance limitations of current VIIs and friction modifiers. Linear followed by non-linear analogs were prepared.

Task Progress: We synthesized and investigated oil-soluble random and diblock copolymers of dodecyl methacrylate (DMA) and IL methacrylates as potential friction- and wear-reducing additives in lubricants. The effect of molecular weight, polymer topology, and counter anion on the friction and wear behavior of the copolymers was studied. The counter anions included bis(trifluoro-methanesulfonyl)imide (TFSI) and dicyanamide (DCA). The performance was gauged against a similar small molecule IL and tertiary amine functional non-IL copolymers having random and block topology. The synthetic pathway to obtain the polymers via controlled polymerizations, with narrow molecular weights and predictable topology/composition, is illustrated in Fig. 2.2b.1.

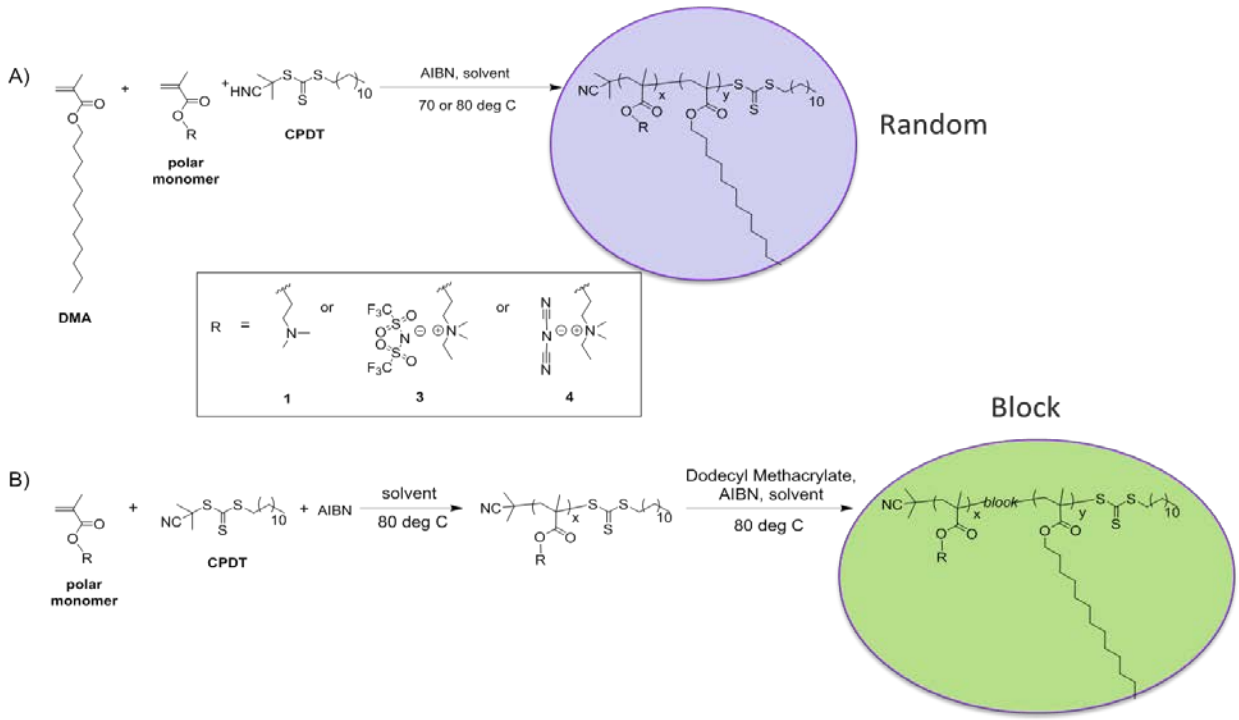

Figure 2.2b.1. Synthetic pathways to copolymers having random and block topology.

The polymers by design had low molecular weight (30-5 kDa) to mimic small molecule behavior. The expectation was that lower molecular weight would yield more resistance towards friction. A modified Plint reciprocating tribometer was used to conduct friction measurements of the test oils. A ball-on-flat geometry was employed. The stationary upper specimen was a hardened type 52100 steel ball with diameter of ½ in, Rockwell scale (Rc) hardness of 62, and Sa of 15 nm. The reciprocating lower specimen was a type 52100 steel (hardened to Rc 62) flat polished to mirror finish (Sa = 6 nm). The testing temperature was 100 °C. The stroke length was 20 mm, and the reciprocation rate was 2 Hz. Tests were nominally one-hour long. A load of 15.6 N was used to produce a peak static Hertzian pressure of 1 GPa. Wear on the ball was calculated by mathematically removing the curvature of the ball.

Figure 2.2b.2 shows the average coefficient of friction at the end of the test and the average ball wear volume for PAO4 samples containing tetradodecylammonium (TDA)-TFSI and all the copolymers. The average ball wear volume for the random copolymers (P1-P5) was consistently lower than that for the block copolymers (P7-P11) having the same composition and molecular weights. This finding indicates that the higher local concentration of the IL repeat units in the block copolymers increased the average wear. This result is contradictory to the expected trend, as these molecules were designed with the expectation that the IL moiety would have a positive effect on wear (i.e., wear reduction). The high wear volume observed for the small-molecule IL control (TDA-TFSI) also indirectly supports this hypothesis. Polymers P5 and P11 containing the DCA counter anion had the lowest wear volume of all the IL copolymers. A direct comparison of random IL copolymers P3 (TFSI) and P5 (DCA), both having similar molecular weights (≈ 10 kDa), indicates that P5 has an average ball wear volume ~85% lower than that of P3. Similarly, comparing the block IL copolymers P11 (DCA) and P8 (TFSI) (≈ 10 kDa, for both) indicates that P11 has an average ball wear volume ~70% lower than that of P8 (TFSI). These results indicate that the counter anion had a remarkable effect on the wear behavior, with the DCA anion providing better wear reduction versus the TFSI anion. A completely opposite correlation between polymer topology and wear volume was observed in the case of amine copolymers P6 and P12. Thus, the average ball wear volume for the block copolymer P12 was ~85% lower than that for the random copolymer P6. These results suggest that a high local concentration of pendant tertiary amine groups in the block copolymer P12 likely promotes effective tribofilm formation, thereby significantly reducing wear, compared to the random copolymer P6.

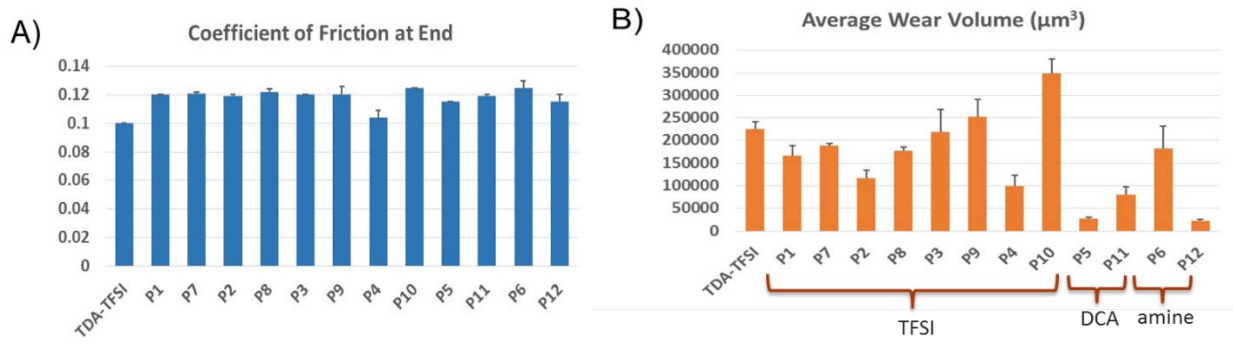

Figure 2.2b.2. Average coefficient of friction at end of testing (A) and average ball wear volume (B) for the control, TDA-TFSI, and polymers P1-P12. Note: the error bars represent standard deviations.

Overall, the results indicate that poly-ionic liquids containing the quaternary ammonium cation do not provide better wear-reduction performance compared to copolymers containing non-ionic polar groups, such as tertiary amines. In contrast to what has been shown before, the lower the molecular weight and the higher the IL content, the higher the wear. This relationship is in complete opposition to what has been reported in the literature (as well as previous work from PNNL) for polymers containing polar moieties that are *not* ionic.

2.2c: Technology Innovation, Design & Synthesis: Multifunctional Colloidal Additives

PIs: O.O. Ajayi and C. Lorenzo-Martin (ANL)

Task Details: This task entailed development of advanced lubricant additive systems that can deliver sustainable friction reduction for extended periods without sacrificing reliability and durability, especially in ultra-low viscosity lubricants. The new additive systems were based on colloidal technology whereby physical and/or chemical mechanisms are used to engineer the surface boundary films with appropriate structure and properties. Comprehensive tribological performance and operating mechanisms of AW, FM, extreme pressure (EP), and thermal control colloidal additives were determined.

Task Progress: To assess the performance of the new colloidal additive systems in relation to current state-of-the-art lubricants, we established friction and wear performance benchmarks with five commercially available advanced engine and gear oils under reciprocating and unidirectional sliding contact. Tests were also conducted with these oils by using standard ASTM four-ball wear test protocol. We formulated FM, AW, EP, and thermal dissipator (TD) colloidal additives. This formulation process involves encapsulation of particulate systems with appropriate surfactant. The various additive systems were blended into ultra-low viscosity synthetic base-fluid (PAO4). Rheological properties were measured in the form of kinematic, HTHS, and cold crank viscosities. All measurements indicated no noticeable change compared to the unformulated base fluid.

Several colloidal additive systems in ultra-low viscosity base fluid were observed to produce friction and wear behaviors comparable to the current advanced benchmark lubricants in both unidirectional and reciprocating sliding, as well as in four-ball tests. Comparative analysis was conducted on the tribofilms from a commercial lubricant and two colloidal additives. The nano-structure of the tribofilms formed from the colloidal additives was similar to the one produced from a current chemical additive system, as shown in Fig. 2.2c.1. These tribofilms consist of amorphous and nano-crystalline mixtures. They all display similar friction and wear behavior consistent with our previous observations that the nanostructure of the tribochemical surface film controls friction and wear under the boundary lubrication regime.

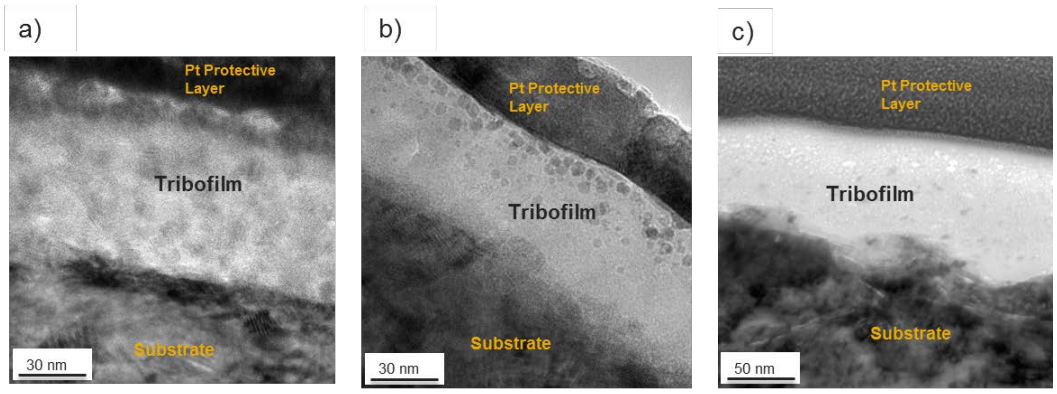

Figure 2.2c.1. TEM micrographs from (a,b) typical colloidal additives and (c) typical fully formulated oil.

Glancing incidence X-ray diffraction (GIXRD) and micro X-ray fluorescence (mXRF) characterization were also conducted on numerous tribofilms at the ANL Advanced Photon Source to determine their structure. These analyses indicated the prominence of Fe_3O_4 and $ZnFe_2O_4$ in surface-protected films from antiwear additives, although without friction reduction. Consequently, a colloidal additive system based on particles of these two oxide structures was formulated. The particles were encapsulated with oleic acid and blended with PAO4 base-stock fluid. Figure 2.2c.2a shows the TEM micrographs of $ZnFe_2O_4$ colloidal particulate components. Friction and wear tests were conducted with these new antiwear additives blended into ultra-low viscosity PAO4 base stock. Under the boundary lubrication regime, the average friction coefficient was about 0.1, which is comparable to fully formulated lubricants under the same conditions. The impact of these new colloidal additives was much more dramatic on wear. Figure 2.2c.2b shows an optical micrograph of the tribofilm formed from $ZnFe_2O_4$ colloidal additive. Profilometry analysis shows the buildup of a 100-150 nm protective tribofilm on the surface, as indicated in Fig. 2.2c.2c.

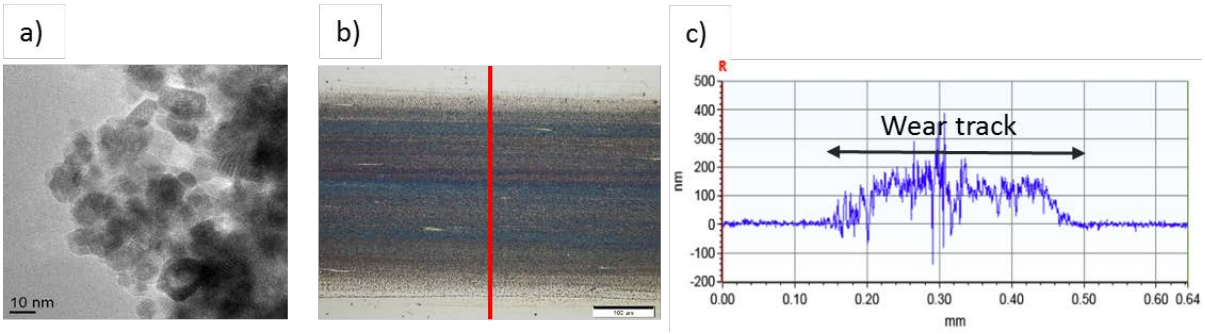

Figure 2.2c.2. (a) TEM image of colloidal particles, (b) optical micrograph of tribofilm, and (c) profilometry of wear track for flat specimen tested with $ZnFe_2O_4$ colloidal additives.

2.3: Technology Innovation, Design & Synthesis: Materials and Coatings (ANL)

PIs: A. Erdemir, O. Eryilmaz, and G. Ramirez (ANL)

Task Details: This task entailed the development of catalyst coatings that can extract self-healing, durable, amorphous carbon boundary films from lubricating oils to achieve 20% reduction in friction without degrading reliability. The architectures of the new nanocomposite coating incorporate metal catalysts that can convert long-chain hydrocarbon oil molecules into slick, durable, and scuff-resistant amorphous carbon boundary films.

Task Progress: The major focus of the coating effort was on the design, synthesis, and characterization of nanocomposite coatings that can reduce friction and wear under severe boundary conditions. Accordingly, the first year's effort concentrated on the development of a series of nanocomposite coatings based on VN-Cu and VN-Ni systems. A CemeCon magnetron ion plating system was used to develop these coatings by optimizing the deposition parameters to achieve a uniform distribution of the hard nitride and soft metallic phases within the coating microstructure. Table 2.3.1 shows the optimized deposition conditions for the synthesis of VN-Cu and VN-Ni coatings used in mechanical and tribological tests. These coatings were fully characterized for their surface roughness, film thickness, nano-hardness, and adhesion. Structurally, optimized coatings displayed a very dense morphology without the existence of any columnar grains or any types of defects or cracks. Surface roughness of the optimized coatings was in the range of 10 to 29 nm, and the nanoindentation tests confirmed the hardness of composite coating to be about 20 GPa (Figure 2.3.1). We also confirmed that this coating had excellent adhesion to the steel substrate with overall adhesion strength of HF1, which is indicative of strong adhesion. Overall, we were able to produce two types of coatings (VN-Cu and VN-Ni) of very high-quality and suitable for tribological testing.

Table 2.3.1. Deposition conditions for VN-Cu composite coating.

Working temperature	250 °C
Target-substrate distance	5 cm
Background pressure	0.0007 Pa
Working pressure	0.4 Pa
Buffer film	<100 nm V+VN_x
Coating thickness	400-1500 nm
Gas flow N_2/Ar (sccm)	78 / 120
V Target HPPMS[a] (power density)	6300 W (14.18 W/cm^2)
Cu target DC power (power density)	80 W (0.20 W/cm^2)

[a] HPPMS = high-power impulse magnetron sputtering.

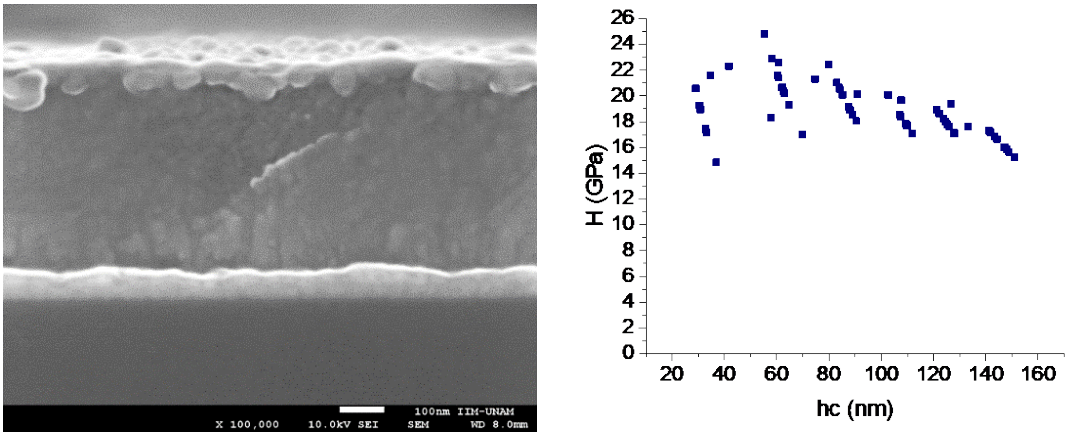

Figure 2.3.1. (a) Cross-sectional morphology of a VN-Ni catalyst coating showing very dense and non-columnar morphology and (b) the nanohardness profile of the same coating confirming high hardness (≈20 GPa).

Initial screening tests for tribological performance were carried out in a high-frequency reciprocating test machine using 10-mm diameter balls (point contact) and cylindrical pins (line contact) under light (0.19 GPa), moderate (1 GPa), and very high (2.38 GPa) contact pressures for 2 hours with a fully formulated oil from Infineum. Anti-friction and -wear additives within this oil appeared to dominate the test results. Hence, the friction and wear coefficients of coated vs. un-coated samples were not much different from one another (Fig. 2.3.2). However, tested in an aged oil with soot, coated surfaces exhibited a noticeable improvement in wear performance but very little difference in the friction coefficient (presumably due to soot and debris contaminants in the oil).

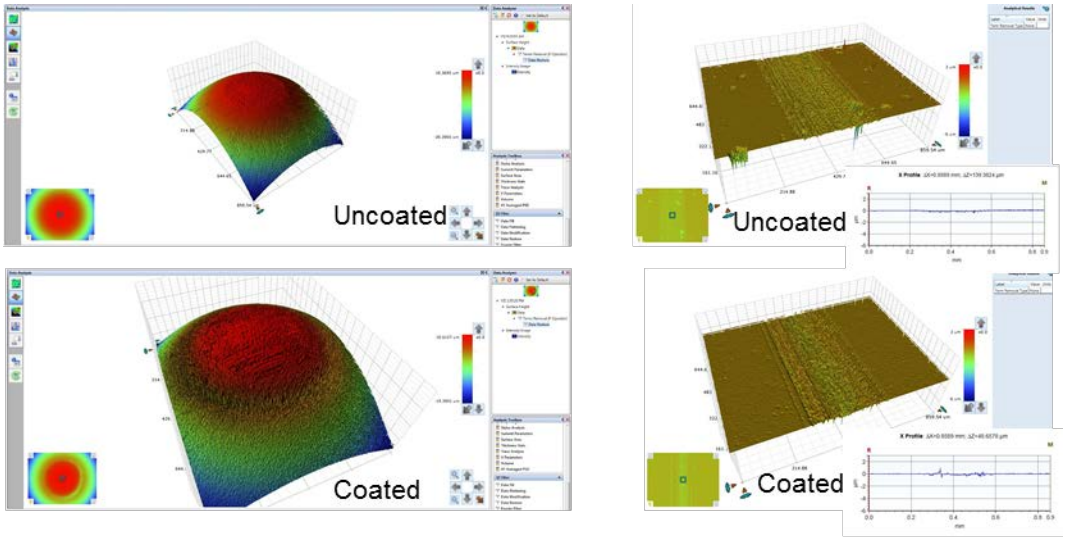

Figure 2.3.2. 3D images of the worn ball surfaces (left) and flat surfaces (right) for both uncoated (top) and coated (bottom) flats.

3. Research Progress: Thrust Area 3 - Lubricant Effects on Combustion and Emissions Control (Thrust Lead: J. Storey – ORNL)

3.1a: Lubricant Effects on Combustion and Emissions Control: Lubricant Effects on PM Emissions (ORNL)

PIs: J. Storey (ORNL)

Task Details: It is critical to understand the contributions of the lubricant to the particulate matter (PM) from gasoline direct injection (GDI) engines as lubricants and direct injection engines evolve to meet new fuel economy requirements. We examined whether components of the lubricant are present in the hydrocarbon fraction of the PM and/or as solid ash particles. The influence of lubricant properties on the size and concentration of PM production during cold start was also investigated.

Task Progress: This task evaluated lubricant effects on PM emissions from a GDI engine during cold start. PM emissions during cold start can be up to ten times higher for a GDI engine than during the warm up portion of the certification cycle. A start cart was constructed to enable multiple starts of an engine. The engine on the cart is a 2.0-L turbocharged GDI engine, and forced cooling was implemented to enable repeated cold starts without a 12-h soak. The apparatus was used to determine the impact of lubricant viscosity on PM production during cold start.

For the PM emissions research, the GDI engine operated on an Environmental Protection Agency (EPA) Tier III certification fuel (E10). Three different oils were studied, each from the same manufacturer but with different viscosities (0W-20, 10W-30, and 20W-50). Since each cold start is only 90-s long, PM samples from 8 cold starts were collected on a single set of filters, and three sets of filters were collected for each lubricant. Quartz filters were used to measure the elemental vs. organic distribution of the carbon fraction (EC/OC) of the PM.[3] Figure 3.1a.1 shows that EC is relatively constant for the three lubricants, but the OC decreases with the highest viscosity lubricant, 20W-50. Lower viscosity lubricants are favored for fuel economy gains, but may contribute to higher PM emissions during cold start.

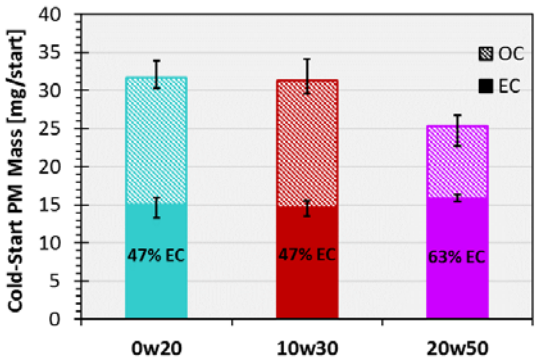

Figure 3.1a.1. Relationship between PM organic and elemental carbon (OC, EC) for the three lubricants evaluated. Points are averages of three filter samples, and error bars span the maximum and minimum values.

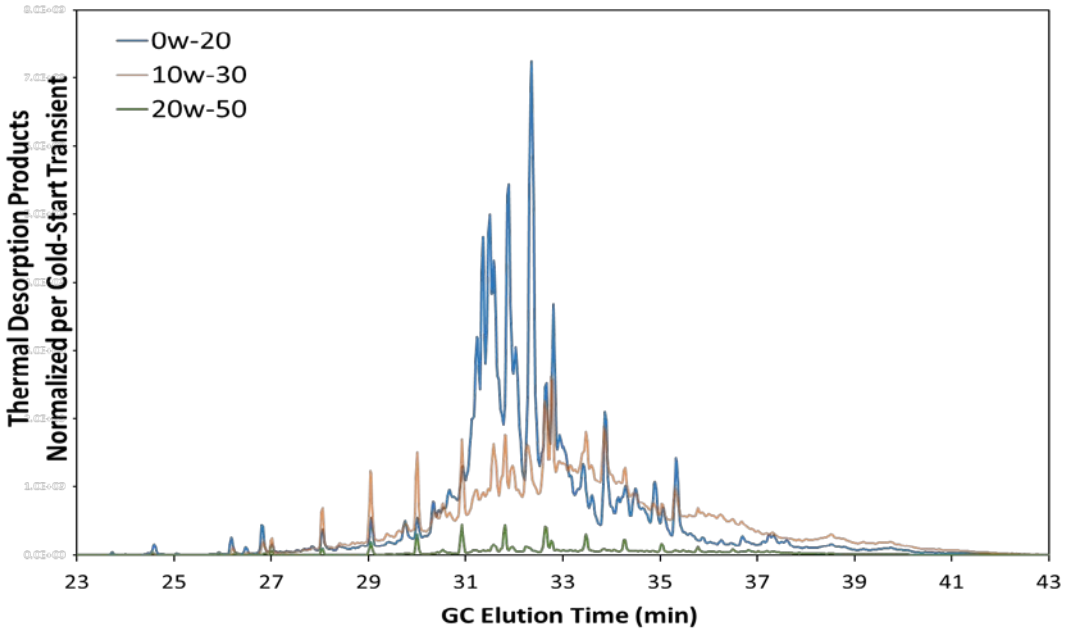

Figure 3.1a.2. Chromatogram of the thermal desorption step for PM collected under cold start conditions from a GDI engine with three different viscosity lubricants. The MS signal has been normalized to the mass of the PM per cold start. The lightest weight oil, 0W-20, has the highest quantity of compounds and the heaviest oil, 20W-50, has the least amount removed by the thermal desorption step.

Filters were also analyzed by thermal desorption pyrolysis/gas chromatography/mass spectroscopy. Although not identical to the OC fraction measured by the National Institute for Occupational Safety and Health (NIOSH) method, the HC fraction resulting from the thermal desorption is a similar, thermally labile fraction of the PM (Fig. 3.1a.1). The speciation of this fraction in Fig. 3.1a.2 thus represents the composition of the OC. Figure 3.1a.2 shows that the 0W-20 has more of a lighter fraction (oil base-stock components) that comes off between 29 and 32 minutes compared to the 10W-30 and 20W-50. In contrast, higher desorption temperatures are required to observe the base stock components for the higher viscosity lubricants.

The results of this study to date contribute to the goal of validating fuel-saving lubricant technologies. Lower viscosity lubricants improve fuel economy. However, lubricants that also contribute excessively to PM mass emissions may need to be modified to avoid these emissions.

3.1b: Lubricant Effects on Combustion and Emissions Control: Lubricant Effects on Emission Controls (ORNL)

PIs: T. Toops (ORNL)

Task Details: As advanced lubricant additives and surface treatments are developed and made ready for evaluation in lubrication systems, it is important to identify the benefits, such as improved fuel economy, and any potential problems, such as impacts of combustion by-products on emissions and emissions control systems. In this report period, benchmarking of baseline lubricants was performed.

The plan was that as lubricant formulations became available through Thrust I and II activities, they would be evaluated within the framework of these tasks.

Task Progress: To understand lubricant effects on emissions controls, rapid aging of three-way catalysts was performed with three additives, and the results compared to those for catalysts that had not been aged or were aged with no lubricant additives, as well as a three-way catalyst from a vehicle at full useful life of 117,000 miles. All of the catalysts adequately removed the criteria pollutants, NO_x, HC, and CO, so the more sensitive water-gas shift (WGS) reaction was used to identify performance degradation. In this reaction, CO and H_2O react to form H_2 and CO_2; WGS activity can indicate abundance of active sites, which can be lost over time due to sintering of precious metals like Pd. Figure 3.1b.1 illustrates the relationship between WGS activity and temperature for the different samples. Prior to the WGS analysis, all of the aged catalysts were de-sulfated in the same way. Figure 3.1b.1 shows that the three-way catalysts exposed to engine exhaust aging with additives lost about 30% of their activity, but the catalyst that was aged on a vehicle lost about 90% of its WGS activity. Most importantly, this approach illustrates that the novel lubricant additive component with IL does not deactivate three-way catalyst functionality more so than the industry standard, ZDDP.

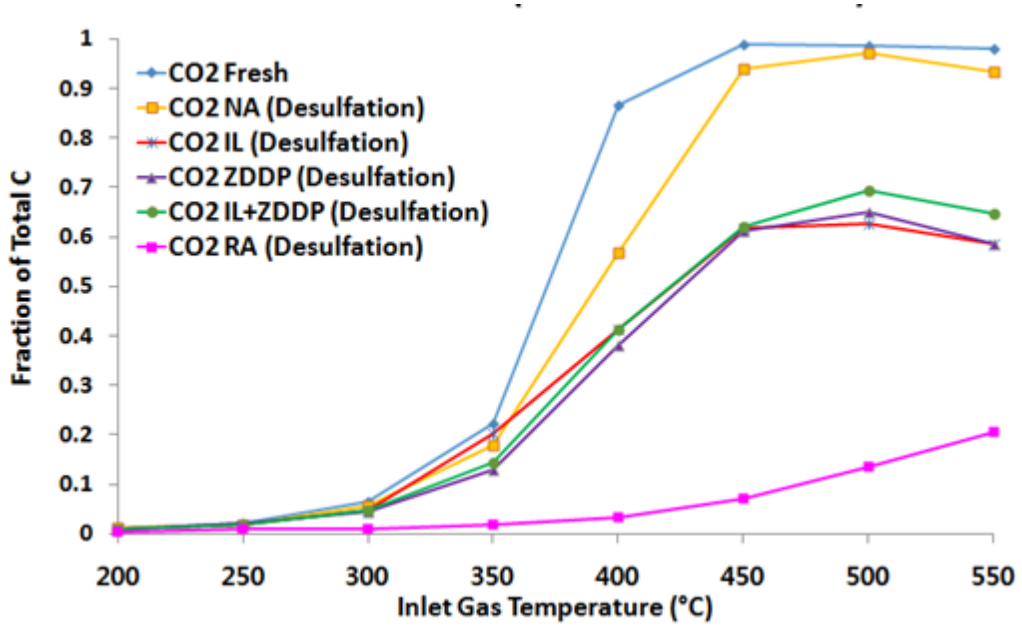

Figure 3.1b.1. Formation of CO_2 in WGS reaction between 200 and 550°C for three-way catalysts aged with different lubricant additives.

The results validate the fuel economy benefits of the IL additive by demonstrating the compatibility of the fuel-saving additive with emissions control. The method further identified a sensitive measure of lubricant additive degradation: 40% reduction in key catalyst sensitivity was observed due to accelerated aging.

3.2a: Lubricant Effects on Combustion and Emissions Control: Lubricant Effects on Low-Speed Pre-Ignition (ORNL)

PIs: D. Splitter (ORNL)

Task Details: Downsized and turbocharged spark-ignited engines are being increasingly used by engine manufacturers to improve vehicle efficiency while reducing CO_2 emissions. While effective at improving fuel economy, the increased specific outputs of these engines makes them more prone to damaging phenomena such as pre-ignition. Although pre-ignition is not a novel process or unique to downsized boosted engines, the high-load low-speed operating conditions of these engines result in a particularly intense pre-ignition process, which is typically referred to as low-speed pre-ignition (LSPI). LSPI events often consist of very strong knock event(s) that can cause significant damage to engine hardware, including catastrophic engine failure.

LSPI typically occurs during very-high load operation at engine speeds around 2000 rpm or below, wherein the flame initiates before the spark is fired and leads to flame propagation at a significantly advanced combustion phasing. The increased pressure rise due to the advanced combustion phasing often causes violent end-gas knock or even "super-knock" for events that transition to developing detonation, all of which can result in catastrophic engine damage. The fundamental causes of LSPI still remain poorly understood, and while there is a lack of firm consensus on the underlying mechanisms that promote LSPI, a strong link to lubricant detergent properties has been found in the literature. Although significant recent work has been undertaken to understand LSPI processes, a gap still exists in the understanding of the source and cause of lubricant properties on LSPI behavior. This project aims to provide more clarity on the relationship between lubricant properties and LSPI, with lubricant additive package properties such as detergent types and formulation being specifically studied.

Task Progress: Activities focused on experimental testing of several lubricants at LSPI-prone conditions. The approach used for these studies differed from conventional LSPI testing. In an effort to reduce engine hardware failure, a fuel with a low octane number was used, 71 RON and 68 MON. Note that this fuel had near identical distillation as compared to previous LSPI prone conditions used in previous ORNL testing for the Co-Optima program. The low octane approach combined prior knowledge in LSPI gained from the previous quarters in that LSPI events are prone at conditions where a steep gradient in ignition delay occurs. Thus, the reduced octane number resulted in a steep gradient in ignition delay occurring at a reduced pressure and thus fueling rate with similar distillation. We found that an LSPI prone condition occurred at approximately 50% less fueling rate than higher load and higher octane conditions. Note that an effort was made to increase the propensity of fuel wall impingement with the reduced fueling rate, which was verified from oil fuel dilution trends being similar between the low and high load conditions. Using this framework, we inferred that the fuel-oil dilution in the top ring zone was similar between the operating loads and fuels. Based on this preliminary testing with close to matched fuel-oil mixing in the top ring zone, we found that when LSPI events occurred, the magnitude of the events was reduced, and engine hardware failure was also reduced.

This reduced octane number approach yielded many SPI events, as the fuel was at a kinetic state that was receptive to LSPI events. However, the LSPI event count was completely insensitive to lubricant type or additive pack; this was unexpected. Multiple lubricant additive packages were tested, where the specific additive packages are shown in Fig. 3.2a.1. Note that a total of five lubricant additive packages were tested.

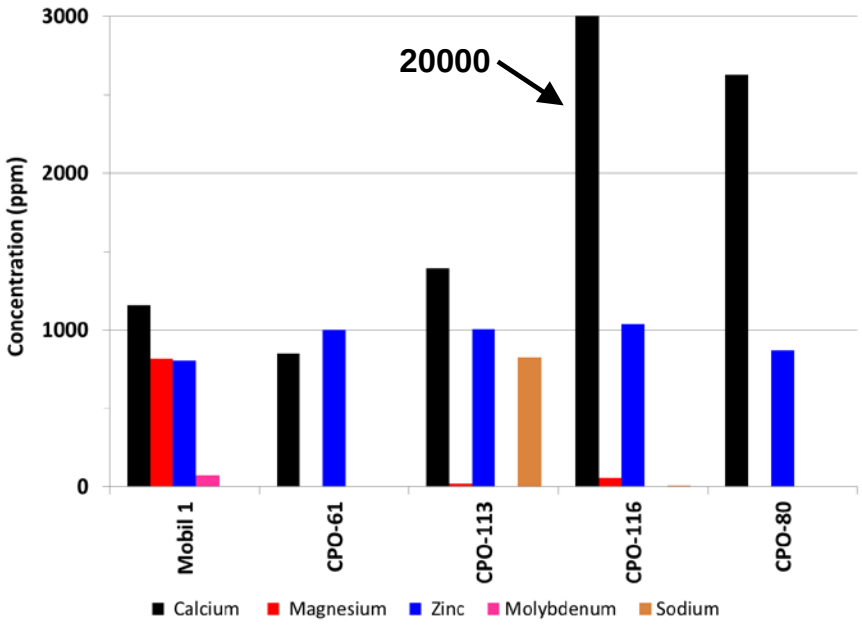

Figure 3.2a.1. Lubricants tested with additive pack metals in tested lubricants. The CPO lubricants are all group 3 base stock; all lubricants are 5W-20 SAE grade. (See Table 3.2b.1 for CPO lubricant compositions.)

The lack of additive package effect on LSPI at this reduced load condition was an interesting finding, as literature trends at higher loads have shown that the lubricant additive package can influence LSPI trends significantly. Specifically, the detergent levels and elements tested in the lubricants in Fig. 3.2a.1 should have generated significant trends in LSPI event count. For example, calcium content in the 2000 ppm range has been shown in several literature reports to have a significant effect in increasing LSPI event count; however, in our testing, not only did a 2600 ppm concentration not have any effect over the baseline lubricant (Mobil 1), but an order of magnitude increase in calcium content (20,000 ppm) also had no measurable effect on LSPI event count. Likewise a sodium-containing lubricant was tested, and this lubricant also had no statistically significant difference in LSPI event count. Again, this finding was unexpected as literature trends had suggested that sodium detergents could be even more prone to LSPI events than calcium detergents. The LSPI trends of the lubricants shown in Figure 3.2a.2 illustrate the average LSPI count per 20 minute segment of testing.

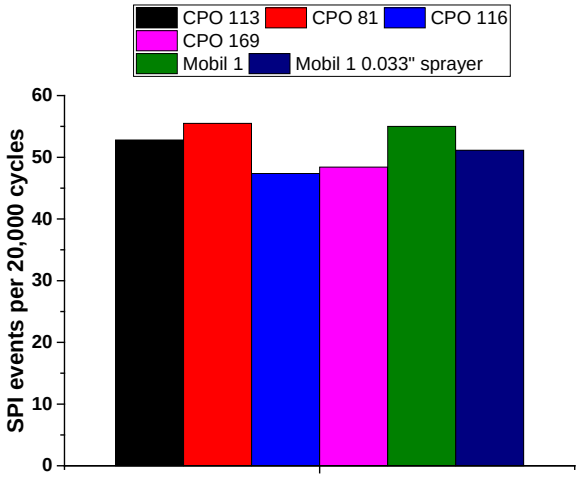

Figure 3.2a.2. Average LSPI event count for various tested lubricants at matched operating condition with 71 RON fuel at SPI prone operating condition. (See Table 3.2b.1 for CPO lubricant compositions.)

The meaning and reason for this unforeseen outcome are not fully determined. The results suggest that for LSPI events to occur there is a thermal factor that influences the lubricant property dependence on LSPI events. The results suggest that new lubricant additives that enable high fuel economy base stocks will need to be evaluated for their tendency to induce LSPI in GDI engines.

3.2b: Lubricant Effects on Combustion and Emissions Control: Lubricant Effects on Low-Speed Pre-Ignition (NREL)

PIs: B. Zigler (NREL)

Task Details: This task supports the ORNL engine work in Task 3.2a, with the goal of correlating LSPI behavior with characteristics determined in constant-volume combustion chamber (CVCC) studies. By mapping ignition delay behavior for lubricating oil/fuel surrogate mixture blends over engine-relevant pressure and temperature space, CVCC studies, in theory, would allow more focused studies on the kinetics of lubricating oil/fuel mixture ignition promoting LSPI than engine studies alone. In addition, if a strong correlation were to be found between a CVCC-based method to identify LSPI-promoting ignition behavior for lubricants, the opportunity exists to develop a simple test for oil reactivity that not only correlates well to LSPI frequency, but is able to offer enough precision to clearly discriminate between the wide variety of lubricating oil samples that exist today. While a CVCC-based test method may never replace engine-based final testing, the ability to conduct initial screening quickly and efficiently (without damaging engine hardware) could augment final approval screening of engine-based lubricating oil.

Task Summary: Activities for this task focused on parametric ignition delay studies of lubricating oil/fuel surrogate blends in a CVCC to evaluate the hypothesis of oil microdroplet ignition initiating the LSPI event. Initial studies were conducted in NREL's highly modified Ignition Quality Tester (IQT), then transitioned to the newer, more flexible Advanced Fuel Ignition Delay Analyzer (AFIDA) platform. While prior parametric (temperature, pressure, and oxygen fraction) studies in the IQT significantly differentiated ignition delay time between base stocks for lubricant/fuel blends, we moved to the AFIDA

(1200 bar injection pressure, piezo injector, and higher pressure and temperature capability) to better simulate microdroplets and engine conditions where the LSPI event is theorized to initiate.

A matrix of fourteen 5W20 oil samples, prepared by ORNL's industry partner and shared by Derek Splitter (ORNL), was formulated from the same PAO group 4 base stock but contained varying amounts of additive elements. These samples were used to determine autoignition differences induced by varying additive package components. The components were boron, molybdenum, phosphorus, zinc, sodium, calcium, magnesium, and tungsten. Five commercial lubricating oils were also chosen to cover a wide range of base-oil categories, additive packages, and performance claims in an effort to make the test matrix meaningful and reproducible. Industry consultation guided the selection of some of these oils to cover a wide range of base-oil categories, additive packages, and performance claims. No attempt was made to determine or divulge the actual composition of the commercial oils, but some basic analyses were performed for qualitative comparison. Table 3.2b.1 shows the matrix of lubricating oil samples used in the CVCC experiments.

Table 3.2b.1. Composition of lubricating oils studied in IQT and AFIDA experiments.

Oil ID	Si	B	Mo	P	Zn	Na	Ca	Mg	W	V100	V40	VI	TBN	Density
Commercial Oils														
A - SuperTech	4	187	24	758	816	<5	2066	12						0.8543
B - Mobil 1	7	107	82	755	815	<5	1106	753	0	8.9	47.6	171	7.01	0.8473
C - Pennzoil Platinum	5	2	63	754	847	<5	2589	10						0.8341
D - Amsoil	5	78	<1	600	666	<5	1421	9						0.8483
E - Redline	6	3	124	740	779	<5	1542	5						0.8763
Additive Oil Matrix														
CPO-61	2		<1	736	853	0	520	14	0	7.3	35.8	175	1.08	0.8266
CPO-81	4		<1	812	999	0	851	1	0	7.7	37	185	1.31	0.8337
CPO-80	<1		<1	769	872	0	2626	0	0	7.6	38.7	169	6.56	0.8334
CPO-64	5		356	740	809	0	2519	8	0	8.3				0.8334
CPO-65	3		2	787	837	0	2577	8	350	8.1				0.8310
CPO-83	5		<1	1017	1210	0	2321	7	0	7.7	39	171	3.02	0.8274
CPO-63	3		24	1121	1279	0	2681	10	0	7.6	39.5	164	6.56	0.8294
CPO-85	3		<1	554	633	0	397	1090	0	7.3	37.3	162	4.28	0.8285
CPO-84	7		<1	816	965	0	22	1528	0	8.3	40	190	6.21	0.8294
CPO-112	3	<1	1	936	1080	0	2301	8	0	7.7	39.2	171	3.36	0.8317
CPO-113	3	3	<1	855	1003	822	1396	20	0	7.7	38	177	4.28	0.831
CPO-114	3	1	<1	799	918	857	24	1024	0	8	38	190	6.44	0.8309
CPO-115	3	1	<1	890	1048	727	709	736	0	7.6	37.6	473	5.53	0.8313
CPO-116	6	<1	1	905	1035	7	20000	55	0	8.8	46	174	21.03	0.8551
Volatility Oil Matrix														
CPO-164	CPO-61 Clone, Low Volatility													0.8266
CPO-165	CPO-80 Clone, Low Volatility													0.8310
CPO-166	CPO-61 Clone, Medium Volatility													0.8198
CPO-167	CPO-80 Clone, Medium Volatility													0.8233
CPO-168	CPO-61 Clone, High Volatility													0.8159
CPO-169	CPO-80 Clone, High Volatility													0.8202

Various experimental trials were conducted (initially in the IQT and later in the AFIDA) to evaluate ignition resistance of lubricating oil/fuel surrogate blends for different fractions of oil to fuel, oxygen fraction, pressure, and fuel surrogate type. In general, high fractions of lubricating oil (75 vol%), low oxygen (10%), high pressure (~30 bar), and para-xylene fuel surrogate (instead of iso-octane) helped show separation between the ignition resistance of the oil samples. However, none of these differences was significant, and most importantly, additive metals did not show significant differences in the IQT or AFIDA. As the project funding was suspended, NREL was beginning to investigate this in more detail; however, a cause was not found. One possibility is that the AFIDA (and IQT) experiments were targeting the wrong experimental conditions (temperature, pressure, and oxygen fraction). However, these same general experimental conditions were used in other Co-Optima project research to study fuel ignition kinetics and were related to experimental studies of knock-limited performance in a boosted SI single-cylinder engine. Another possibility is that the AFIDA experiments were correctly indicating that lubricating oil composition with respect to metal additives had no significant effect on ignition delay for these oil/fuel mixtures. Coupled with ORNL's similar engine studies of LSPI (Task 3.2a), this finding may indicate that other factors govern initiation of LSPI, factors that were not present or isolated in the AFIDA experiments.

To test that the AFIDA-based parametric ignition delay measurements related to engine-based LSPI experiments, ORNL shared experimental data concerning an LSPI event from Task 3.2a with NREL. NREL had not completed those correlations at the time of this writing, but intends to do so by 31 July 2018 to complete a delayed milestone. This work is based on a similar Co-Optima task to correlate AFDIA-based ignition delay surface maps with boosted SI engine data, using a knock integral calculation. A 0D simulation model was developed in Python to import SCE crank-angle resolved cylinder pressure and intake pressure data and calculate cylinder temperature prior to spark ignition. The engine simulation is a two-zone model calculating both unburned and burned fractions to match ORNL's experimental cylinder pressure data. The unburned fraction temperature and cylinder pressure were simultaneously fed to a modified Livengood-Wu knock integral calculation with a Douaud and Eyzat correlation to calculate autoignition (triggering the greater LSPI event) using interpolations from the AFIDA pressure/temperature space ignition delay data. The results of this bridging simulation can be used to evaluate whether the existing AFIDA-based ignition delay data predict any early-stage LSPI-inducing event in ORNL's supplied engine pressure trace.

3.3: Lubricant Effects on Combustion and Emissions Control: Lubricant Effects on Fuel Economy in Vehicle Experiments (ORNL)

PIs: B. West (ORNL)

Task Details: The task objective was to develop a method for rapidly assessing the impacts of improved lubricating oils on vehicle fuel efficiency to support programs aimed at improving the fuel economy of both emerging and legacy vehicles. The goal is to bridge the conventional Sequence VI test results to "real world" fuel economy results (mpg).

Task Progress: Vehicle-level fuel economy has been measured on four vehicles in this project, as seen in Fig. 3.3.1. Vehicles include a Cadillac SRX (which is equipped with the same DOHC 3.6 GDI engine that is used in the ASTM Sequence VID test), a Chevrolet Silverado V8, a Nissan Frontier with inline four-cylinder engine, and a late model BMW 320i with a 4-cylinder turbocharged GDI engine. All experiments anchor measurements of test lube fuel economy against the same test protocol with the ASTM Base Lube. Test lubricants have included Mobil 1 5W-30 engine oil and a prototype lubricant from PNNL, and

sequence test results have been acquired for Mobil 1 and the prototype PNNL lubricant. Statistically significant fuel economy differences of 1-5% were measured in the vehicle laboratory with all four vehicles and engine architectures using the transient city fuel economy and highway fuel economy tests, as well as a custom quasi-steady test with cruise conditions from 40 to 80 mph. These three test cycles combine to cover the majority of the vehicle operating map, as opposed to the Sequence VI test.

Figure 3.3.1. Vehicles installed on chassis dyno for fuel economy testing.

Fuel economy improvement for the four vehicles with 5W-30 engine oil is shown in Fig. 3.3.2 for each phase of the urban driving cycle known as the Federal Test Procedure (FTP), the highway driving cycle (HFET), and nine steady-state cruise speeds. The most significant fuel economy improvement for any test lubricant is for Bag 1 of the FTP. This portion of the test consists of the first 505 seconds of the FTP. The test begins at room temperature; thus, the relatively cold lubricant has higher viscosity, and the 5W-30 test lubricant provides the greatest fuel economy improvement as compared to the 20W-30 ASTM base lubricant, on the order of 3-5%.

Bag 2 of the urban cycle is on a relatively warm engine, and the drive cycle for Bag 3 is identical to Bag 1 except it is run after a 10-min rest period; the engine and oil are still quite warm for the Bag 3 test. For the warm Bag 2 and Bag 3 results, the average benefit drops to less than 2-3%. The HFET is a light load test conducted on a warm engine. Fuel economy improvement on the HFET ranges from 1% to 2%.

The steady-state driving results also range from 1% to 2%, with the greatest improvement at the lower speeds. Similar to the HFET, the steady-state tests are conducted on a warm engine. It is interesting to note that the difference between the base and the test lubricant is largest at the low speeds. The required engine power increases dramatically with increasing wheel speed. Because engine friction is a larger fraction of the total power at the slower speeds, the fuel economy difference for a lower viscosity oil is more apparent at the lower speeds.

The results across the various cycles for these four vehicles are fairly consistent, despite all having different engine architectures, representing a high-feature DOHC V6, a pushrod V8, an inline 4-cylinder, and a late-model turbocharged, direct-injection four cylinder.

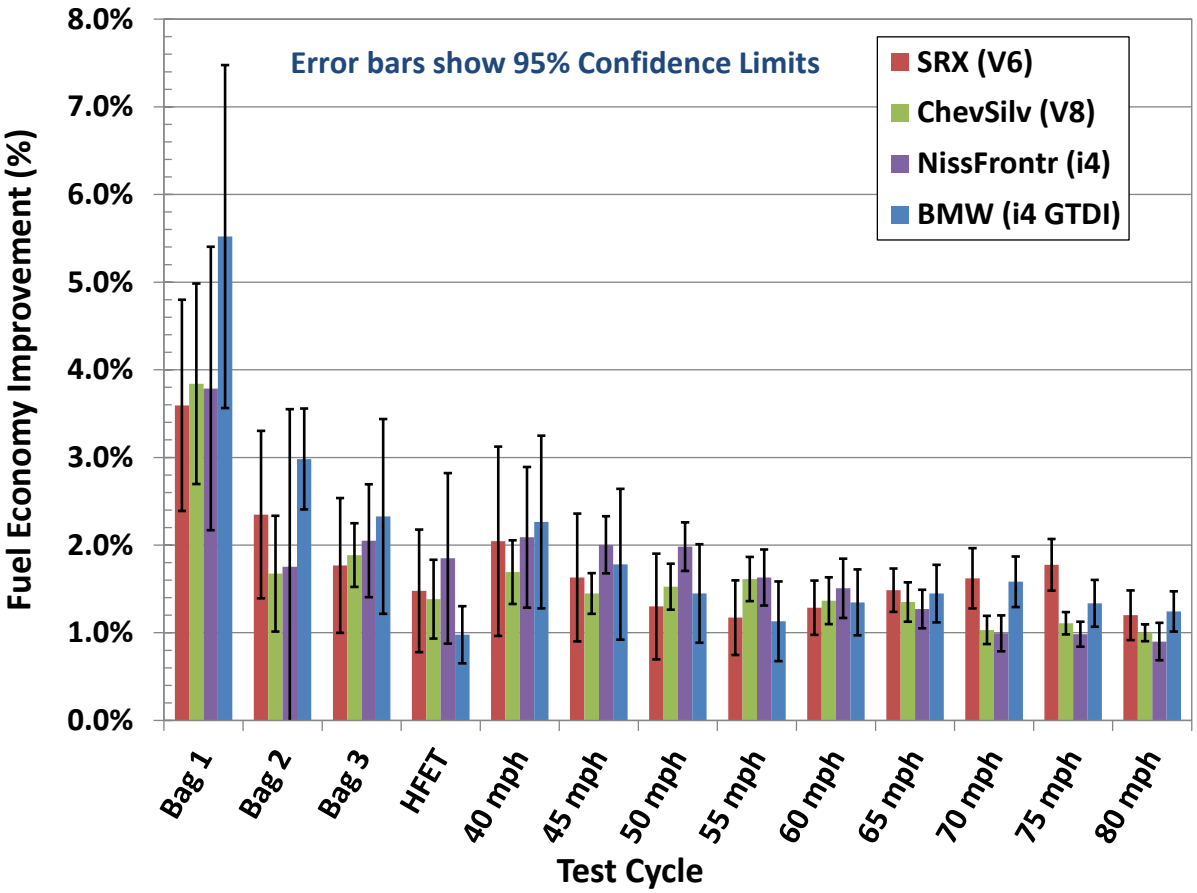

Figure 3.3.2. Fuel economy Improvement by test cycle for four vehicles with 5W-30 test lubricant compared to ASTM base lubricant.

Acknowledgements

This work was supported by the U.S. Department of Energy, Office of Energy Efficiency and Renewable Energy, Vehicle Technologies Office, Advanced Combustion and Fuels R&D, Fuels & Lubricants Program. The authors and PIs wish to express their appreciation to Dr. Michael Weismiller (Technology Manager) for his continued support and encouragement on this project.

Applied Materials Division
Argonne National Laboratory
9700 South Cass Avenue, Bldg. 362
Argonne, IL 60439

www.anl.gov